Post-Fire Soil Erosion Patterns and Processes in a Complex Sagebrush Rangeland Watershed

A Thesis

Presented in Partial Fulfillment of the Requirements for the

Degree of Master of Science

with a

Major in Water Resources

in the

College of Graduate Studies

University of Idaho

by

Samantha Pauline Vega

Major Professor: Erin S. Brooks, Ph.D.

Committee Members: Frederick B. Pierson, Ph.D.; Christopher J. Williams, Ph.D.;

Eva K. Strand, Ph.D.

Departments Administrator; Robert Heinse, Ph.D.

August 2018

Authorization to Submit Thesis

This thesis of Samantha Pauline Vega, submitted for the degree of Master of Science with a Major in Water Resources and titled "Post-Fire Soil Erosion Patterns and Processes in a Complex Sagebrush Rangeland Watershed," has been reviewed in final form. Permission, as indicated by the signatures and dates below, is now granted to submit final copies to the College of Graduate Studies for approval.

Major Professor: _____ Date: _____

Erin S. Brooks, Ph.D.

Committee Members: _____ Date: _____

Frederick B. Pierson, Ph.D.

_____ Date: _____

Christopher J. Williams, Ph.D.

_____ Date: _____

Eva K. Strand, Ph.D.

Department

Administrator: _____ Date: _____

Robert Heinse, Ph.D.

Abstract

Across the western United States, wildfires in sagebrush vegetation are occurring at a more frequent rate and higher intensity. Erosion following wildfire is a main concern among land managers due to the threat it poses to resources, infrastructure, and human health. The purpose of this study is to improve scientific understanding of how site physical and biological attributes effect hillslope to watershed scale sediment yield on a mountainous burned sagebrush landscape. The north-facing aspect produced more erosion post-fire due to the combination of soil, topographic characteristics, and vegetation cover pre- and post-fire. The drivers for both years post-fire was mainly wind and winter season runoff processes rather than summer thunderstorms. This study found that substantial erosion can be driven by combined wind and water processes post-fire. These results highlight the control site characteristics have on a landscapes hydrologic and erosion response and the risk winter processes pose to burned landscapes.

Acknowledgements

I thank my University of Idaho Committee members for their mentorship and support throughout my field work, data analysis, and writing. I have enjoyed working with my advisor Dr. Erin S. Brooks. His mentorship and support has been helpful throughout all stages of my project. I have learned a lot from him during this process and appreciate all the guidance he has given me. I thank Dr. Frederick B. Pierson of the USDA, Agricultural Research Service, Northwest Watershed Research Center (USDA-ARS-NWRC) for providing me with opportunities and for his mentorship. His support has been crucial in all stages of my research. I thank Dr. Christopher J. Williams of the USDA, Agricultural Research Service, Southwest Watershed Research Center for his mentorship and contribution to field work. His insight and expertise has been extremely helpful when I had questions. I thank Dr. Eva K. Strand of the University of Idaho for helping me with the interdisciplinary component of my project. Her insight was very much appreciated in times of confusion. I thank Dr. Mariana Dobre of the University of Idaho for her contribution to the interdisciplinary component of this project. Her knowledge and collaboration involving running the Random Forest model was a key component. The installation of silt fences was made easier by the guidance of Dr. Peter Robichaud and Robert Brown of the USDA, Forest Service, Rocky Mountain Research Station, Moscow Forestry Sciences Laboratory. I thank Kyle Lindsay previously at the USDA-ARS-NWRC who played a major part in the installation of the silt fences and data collection. I thank Dr. Mark Seyfried of the USDA-ARS-NWRC for his support and field help from staff members Tisha Farris and Mark Murdock. I thank collaborators Dr. Jennifer Pierce of Boise State University and Dr. Kathleen Lohse of Idaho State University for the field help I received from their staff Clay Roehner and Nicholas Patton and for particle size analysis of my samples. I thank Brooke Hansen of the USDA-ARS-NWRC for all her support and lending me staff to help with field work. My field work would not have been possible without the help of Barry Caldwell and Zane Cram of the USDA-ARS-NWRC. I thank Dr. Pat Clark and Alex Boehm of the USDA-ARS-NWRC for crew members to help with field work. I thank Dr. Aaron Fellows of the USDA-ARS-NWRC for his support, friendship, and help with field work.

Dedication

I dedicate this to my friends and family that have supported me throughout my education. This would not have been possible without your love and support.

Table of Contents

List of Figures

List of Tables

CHAPTER 1: REVIEW OF EROSION PROCESSES

1.1 Introduction

Across the western United States, sagebrush rangelands are experiencing burning at a more frequent rate and these fires are commonly larger and of greater severity than for historical fire regimes in these ecosystems (Whisenant 1990; Monsen 1994; Keane et al. 2009; Littell et al. 2009; Miller et al. 2011; Balch et al. 2013). This can be attributed to sagebrush steppe communities having experienced extensive grazing and changing climate conditions making it susceptible to invasion of various invasive plant species (Knapp 1996; Davies et al. 2011; Miller et al. 2011; Balch et al. 2013; Chambers et al. 2014). The annual area burned on sagebrush rangelands has increased in recent decades due in part to an approximate 10-fold reduction in the fire return intervals across much of the sagebrush domain (Whisenant 1990; Keane et al. 2009; Miller et al. 2011; Balch et al. 2013). This increase in wildfire activity has caused a decline in native plant species, an increase in invasive species, and a reduction in habitat for wildlife that rely on sagebrush steppe habitats, such as the greater sage-grouse (Chambers et al. 2014).

Sagebrush steppe communities have declined since early European settlement (Knick et al. 2003). This decline is due to the conversion of sagebrush steppe to annual grasslands as the result of invasive species (Whisenant 1990). Invasive species can severely alter these communities by increasing the amount of fine fuels on the surface, resulting in more continuous fire (Knapp 1996). The exotic annual grass that is the most extensive is cheatgrass (*Bromus tectorum*) (Pellant 1990; Miller et al. 2011). Cheatgrass was first introduced around the early 1900's (Mack 1981; Knapp 1996; Miller et al. 2011; Chambers et al. 2014). Cheatgrass establishes in late spring and relies on spring precipitation. In contrast sagebrush steppe species grow in mid-late-spring and rely on summer precipitation (Bradley 2009). Both plant species capitalize on available resources at different times, which provides differing competitive advantages that may favor the establishment of one species over the other. Cheatgrass can out-compete perennial grasses and fill in interspaces (Mack 1981; Whisenant 1990). Following wildfires high amounts of precipitation in the summer months provide perennial grasses a chance to compete with cheatgrass whereas, during drought conditions

cheatgrass is favored to establish (Bradley 2009). Big sagebrush is impacted by the magnitude and length of drought (Meyer 1994).

Climate models aid in predicting the expansion of invasive species. Climate models indicate that there will be an increase in temperature during the summer months within the Great Basin along with increased precipitation rates in the winter months (Abatzoglou and Kolden 2011; Bradley et al. 2016). These predicted climate trends imply that cheatgrass expansion will continue to increase while increasing the frequency of fire (Abatzoglou and Kolden 2011; Miller et al. 2011; Bradley et al. 2016). Link et al. (2006) confirmed a relationship between potential fire risk and cheatgrass cover. The study found that the probability of fire was <60% when cheatgrass cover was <20%, but the probability of fire increased to 60-86% where cheatgrass cover was 40-60% (Link et al. 2006).

Woodland encroachment by pinyon (*Pinus spp.)* and juniper (*Juniperus spp.)* into sagebrush steppe is also increasing the risk of high severity fires. Woodlands have also expanded over the last 130 years into high elevation sagebrush ecosystems (Miller et al. 2005; Romme et al. 2009; Davies et al. 2011). Over 29 million ha in the western United States are now dominated by pinyon and juniper woodlands (West 1999; Miller et al. 2005). Most woodlands have not been exposed to wildfire for 80-140 years (Keane et al. 2009). The lack of fire in woodlands has allowed for further expansion of pinyon and juniper (Tausch 1999; Heyerdahl et al. 2006). As a result, these landscapes have become more susceptible to crown fires associated with an increase in fuel loading and ladder fuels (Miller et al. 2005). The changes in the fuel loads are a direct result of converting sagebrush steppe into a tree dominated landscape, often with cheatgrass (Miller et al. 2005). The more fuel available for a wildfire facilitates a higher severity fire and a larger fire (Miller and Tausch 2000).

Erosion following wildfires is a concern among land managers due to the threat it poses to natural resources, infrastructure, human health, and safety (Pierson et al. 2011; Williams et al. 2014). Wildfire impacts water quality, carbon storage, runoff and erosion rates, and communities (Ice et al. 2004; Moody et al. 2013). As the number of wildfires increases there is a need to research the impacts fire has on hydrologic and erosion processes. Wildfire effects at the watershed scale have not been researched to the extent that the hillslope

scale has been researched. This can be attributed to the difficulties with instrumentation, assessing the recovery period, and the overall spatial variability of environmental characteristics at the watershed scale (Shakesby and Doerr 2006).

1.2 Fundamentals of Erosion Processes

Erosion of soil by water occurs in two primary forms: inter-rill and rill erosion. Inter-rill erosion is primarily driven by rainsplash and sheet flow or a combination of the two (Bryan 2000; Pierson and Williams 2016). Rainsplash and sheet flow are the dominant processes at fine spatial scales (<1 m^2 to several m^2; small plot scale) with erosion rates depending in large part on the mount of bare soil, soil erodibility, and the erosive energy of rainfall (Nearing et al. 2011; Nouwakpo et al. 2016; Pierson and Williams 2016). Rainfall erosion is the result of rainsplash energy (Bryan 2000; Kinnell 2005). When a raindrop hits the surface, its energy is distributed to wetting, deformation, breaking apart soil particles, and moving the particles up and away (Bradford et al. 1987; Bryan 2000; Kinnell 2005; Pierson and Williams 2016). The impact of the rainsplash energy is the result of rainfall intensity. During high intensity rainfall, rain drops can detach soil particles and redistribute them by particle size. This can lead to surface sealing. Surface sealing is the result of fine material filling pore space on the soil surface and creating a crust (Bradford et al. 1987; Pierson and Williams 2016). This process can increase sheet flow and reduce infiltration rates. Runoff as sheet flow is a method of sediment transportation and detachment (Kinnell 2005; Pierson and Williams 2016). Sheet flow flowpaths are often separated by surface obstacles creating isolated patches of flow (Pierson and Williams 2016).

Rill erosion is driven by concentrated flow that produce microchannels. This occurs at large-plot scales (tens of square meters), and the sediment yield produced by rill processes is much larger than that by inter-rill processes (Pierson and Williams 2016). Microchannels are the result of surface roughness or flow accumulation concentrating sheet flow, resulting in deeper flow paths, faster flow velocity, and increased runoff and erosion (Bryan 2000; Pierson and Williams 2016). Concentrated flow is a method of transport for sediment that has been detached by inter-rill erosion processes and can also be a method of detachment (Nouwakpo et al. 2016). Sediment detachment by rill processes occurs when the inter-rill sediment load is

less than the concentrated flow transport capacity and shear stress acting on the soil is greater than the soil surfaces critical shear stress (Pierson and Williams 2016). Sediment deposition of rill transported sediment occurs when the concentrated flow transport capacity is exceeded (Pierson and Williams 2016).

Sediment delivered across spatial scales is the result of interacting runoff-erosion processes, inter-rill-rill processes at the hillslope scale and inter-rill, rill, and channel processes at the watershed scale. The erosion processes that occur at the hillslope scale impact the amount of sediment within a stream channel. Soil particles from hillslope inter-rill and rill erosion can be potentially deposited downhill, on terraces, within vegetation, or into a channel (Ffolliott et al. 2013). Soil particles deposited to the channel can be transported downstream or accumulate in the channel until it moves downstream (Ffolliott et al. 2013). This is called sedimentation. When the water and sediment travel from high elevation to low elevation the stream releases energy by friction and work (Ffolliott et al. 2013). This work applied on the channel and sediment causes the stream channel to change resulting in channel erosion (Ffolliott et al. 2013).

Some of the sediment within the streamflow will be transported out of the watershed during runoff generating precipitation events (Ffolliott et al. 2013). These soil particles can be transported if the settling velocity is lower than the buoyant velocity of the eddies (Ffolliott et al. 2013). This is known as suspended load. The soil particles are generally easily suspended due to their size. Whereas, larger soil particles are transported downstream by saltation, meaning the sediments roll across the bottom of the channel (Ffolliott et al. 2013). During high streamflow events there is a relationship between discharge and suspended sediment. When discharge increases more sediment is transported out of the watershed and when discharge decreases so do the sediment concentrations.

1.3 Impact Wildfire Has on Erosion Processes

Wildfire changes the hydrologic response of a landscape. The results of these changes can be seen at different spatial scales. Wildfire impacts the hydrologic cycle and key factors that can amplify soil erosion processes at the hillslope and watershed scales (DeBano et al. 1996; Shakesby and Doerr 2006; Pierson and Williams 2016). Wildfire impacts on site

hydrologic response to a storm are largely determined by the degree in which fire alters existing vegetation and soils and can be exacerbated or mediated by post-fire climate and the strength and connectivity of water repellent soil conditions (DeBano et al. 1996; Shakesby and Doerr 2006).

When a hillslope is burned portions of protective vegetation and ground cover are consumed by the fire and there is an increase in the amount of ash available for erosion (Shakesby and Doerr 2006). Interception rates decrease with respect to burn severity and vegetation loss. This increase in exposure amplifies rainsplash erosion, sheet flow, and concentrated flow (Bradford et al. 1987; Kinnell 2005; Shakesby and Doerr 2006; Al-Hamdan et al. 2012; Nouwakpo et al. 2016). In addition to removing surface cover wildfire alters the surface topography and soil structure to the extent that the dominant erosion process can shift from inter-rill to rill erosion (Pierson et al. 2011; Pierson and Williams 2016). The spatial connectivity on a hillslope increases following a disturbance like wildfire due to the vegetation being removed therefore decreasing the number of flow obstructions. As result the soil surface is more exposed to erosion by rainsplash or wind. Where ground cover is scarce, flow easily accumulates and concentrates into continuous flow paths and increases soil erosion via rills (Nouwakpo et al. 2016). When hillslope processes are well connected and mixed with bare soil, runoff and soil loss increase (Williams et al. 2016b).

Wildfire can alter infiltration, evapotranspiration, water repellency, and surface sealing, which impact overland flow at the hillslope scale and annual and peak streamflow at the watershed scale (Ice et al. 2004; Shakesby and Doerr 2006). Burned watersheds typically have the highest peak discharge during short high intensity rainfall on steep slopes burned at a high burned severity with increased soil water repellency (Robichaud et al. 2000). Post-fire sediment yields at the watershed scale are the result of precipitation input, burn severity, erosion processes, source of sediment, and watershed size (Smith et al. 2011). Precipitation events following wildfire and rapid snowmelt can amplify stream sediment as the result of increased runoff and erosion (Ice et al. 2004). Post-fire runoff and stream sediment can have a negative impact on water quality and fish habitat downstream (Ice et al. 2004). Wildfire removes vegetation in the riparian area which impacts stream oxygen levels and water

temperature (Ice et al. 2004). The increase in debris and sediment post-fire can also create pooling in the stream again impacting water temperature (Ice et al. 2004).

Fire-induced increased sediment yield at the watershed scale typically declines as a watershed recovers (Shakesby and Doerr 2006). However, it is noted that the fire-induced increase can last a long period of time under certain conditions (Smith et al. 2011). At the watershed scale there is more potential for sediment storage compared to the hillslope scale and often this is reflected in lower measured watershed-scale sediment yields compared to hillslope-scale sediment yields (Shakesby and Doerr 2006). Quantifying sediment processes over the watershed scale is challenging given the spatial variability in erosion and deposition and the lag time for flushing stored sediment from deposition zones.

1.4 Methods of Measuring and Predicting Post-Fire Erosion

Most post-fire erosion research has used rainfall simulator and overland flow experiments (Pierson et al. 2011; Williams et al. 2014; Pierson and Williams 2016). Simulations conducted at fine spatial scales are commonly used to quantify inter-rill runoff and erosion rates. Rainfall simulations conducted over larger spatial scales (10's of m^2) quantify runoff and erosion from combined inter-rill and rill processes. Concentrated overland flow experiments are also commonly employed to quantify runoff and erosion rates and flow hydraulics associated with rill processes. Both rainfall simulations and concentrated flow experiments allow one to control the rainfall or water application rate and minimize variability associated the timing, intensity, and duration of natural storms and, depending on the experimental design, allow for limiting variability in other site physical or biological attributes (Simanton et al.1986).

Rainfall simulation and overland flow experiments have been extremely useful in improving understanding of infiltration, runoff, and erosion processes across multiple spatial scales and in the development of hydrologic and erosion parameters in predictive technologies (Robichaud et al. 2007b; Robichaud et al. 2010b; Al-Hamdan et al. 2012; Pierson and Williams 2016; Hernandez et al. 2017). Rainfall simulators are designed to replicate the intensity and drop size of natural rainfall. Many of the rainfall simulators available can

simulate natural rainfall characteristics (Moody et al. 2013; Williams et al. 2014; Pierson and Williams 2016). However, rainfall simulators have some limitations including difficulties associated with mimicking natural rainfall energies and within-storm intensity variability (Simanton et al. 1986). Nevertheless, rainfall simulators have been an effective tool in assessing fire impacts on hydrology and erosion processes.

Another method of measuring hillslope erosion is the use of silt fences. Silt fences are considered one of the most effective methods to measure hillslope erosion (Dissmeyer 1982; Robichaud and Brown 2002). A silt fence is a synthetic geotextile fabric that is attached to metal or wooden post (Figure 1.1) (Sherwood and Wyant 1976; Britton 2001; Robichaud and Brown 2002). Successful silt fences separate soil particles from runoff and allow them to settle within and in front of the fabric (Theisen 1992). This deposition of soil in front of the fence and within the fence material reduces waters ability to flow through resulting in ponding and the settling of fine to coarse sediment (Sherwood and Wyant 1976; Theisen 1992; Britton 2001). Silt fences are cost effective and allow one to monitor post-fire erosion responses over the first 3-5 years (Sherwood and Wyant 1976; Dissmeyer 1982; Robichaud and Brown 2002). Spigel and Robichaud (2007), conducted a study following the 2000 Valley complex fires that occurred in Montana. They installed 24 silt fences, six fences in each of the four research sites. They found that 75% of the first-year hillslope erosion was driven by rainfall intensity (Spigel and Robichaud 2007).

Past erosion studies have found sediment yields that vary from 0.01 to more than 110 Mg ha^{-1} $year^{-1}$ within the first year after wildfire (Robichaud et al. 2000). Erosion rates typically decrease as vegetation and ground cover returns in the years following fire (Robichaud et al. 2000; Pierson et al. 2001; Robichaud 2005; Pierson et al. 2008; Williams et al. 2016a). Generally increased plant cover on the surface results in greater soil protection from precipitation events. In a prescribed fire study, Williams et al. (2016a) found that erosion was highest one year after fire and returned to pre- fire conditions after five years. The amount of time it takes for a site to recover is influenced by burn severity, pre-fire vegetation, and post-fire weather conditions. DeBano et al. (1996), states that the sediment yields from low severity fires recovered to pre-fire conditions in three years where as moderate-high

severity fires recover within 7-14 years following the fire. A common trend in past research is that erosion may increase directly following fire and then decreases as vegetation grows back and water repellency decreases. In the study of post-fire erosion, disentangling relationships in site characteristics and drivers of post-fire erosion remains limited for rangeland landscapes (Williams et al. 2014).

Figure 1.1. Silt fences are used as a method to measure hillslope erosion. This silt fence was assembled using synthetic geotextile, wooden posts to stabilize the fence, and sod staples to secure the silt fence to the ground surface.

Technologies to predict post-fire erosion at the hillslope and watershed scales have substantially improved in recent years, and there is a suite of prediction models available that are useful in guiding post-fire runoff and erosion mitigation. When it comes to estimating post-fire erosion the Forest Service Water Erosion Prediction Project (FSWEPP) interface encapsulates many of the tools available. The interfaces used in predicting post-fire erosion include Disturbed Water Erosion Prediction Project (WEPP), Erosion Risk Management Tool (ERMiT), and GeoWEPP (Robichaud and Ashmun 2013). Other tools available are the Automated Geospatial Watershed Assessment (AGWA) and the Rangeland Hydrology Erosion Model (RHEM) (Goodrich et al. 2005; Nearing et al. 2011).

Disturbed WEPP predicts mean annual runoff, depth erosion rates, sediment yields, and probability of erosion 1-year post-fire (Robichaud and Ashmun 2013). ERMiT uses

WEPP technology to predict the probability of sediment yield for given burned or recovering hillslopes. Users can simulate rehabilitation treatments to hillslopes to predict treatment success and erosion rates of treated and untreated hillslopes (Robichaud et al. 2007a; Robichaud and Ashmun 2013). GeoWEPP can run in two modes, flowpath and watershed. GeoWEPP predicts runoff and erosion for pixels in the flowpath mode and runoff, peak flow, hillslope sediment delivery to stream for a watershed (Robichaud and Ashmun 2013). AGWA is a GIS based too used to run and build distributed hydrological models. AGWA was created to predict the impact wildfire could have on runoff and erosion (Goodrich et al. 2005). This tool allows the user to perform pre- and post-fire assessments using two watershed hydrologic models, the Soil and Water Assessment tool (SWAT) and the KINematic Runoff and EROSion Model (KINEROS2) (Goodrich et al. 2005). The SWAT model is used for large watersheds and is a continuous simulation model. While KINEROS2 is for small watersheds (arid, semi-arid, and urban), and is an event driven model (Goodrich et al. 2005). RHEM is a modified version of WEPP and is a processed-based erosion model that predicts event-based runoff and erosion rates (Nearing et al. 2011). RHEM was developed to determine run-off, soil erosion rate, sediment delivery rate, and the volume of rainfall from events (Al-Hamdan et al. 2015; Hernandez et al. 2017).

As sagebrush steppe communities experience fire at a more frequent rate and increased size the need for post-fire research is crucial. It is important to further our scientific understanding of how a landscape responds to wildfire and the drivers of erosion post-fire. Past research has made great advancements in understanding the impact fire has on erosion processes, but knowledge is still limited by methods and scaling issues. There are numerous prediction models available that aid in guiding post-fire runoff and erosion mitigation. However, these prediction models largely address warm season thunderstorm events and don’t depict cold season processes that can drive erosion and combined wind and water processes post-fire.

CHAPTER 2: POST-FIRE EROSION DRIVEN BY OVER WINTER PROCESSES

2.1. Introduction

Much of western United States is in the form of rangelands, which occupies roughly 308 million ha (Havstad et al. 2009). Sagebrush steppe represents one of the largest rangeland ecosystems, historically consisting of 63 million ha (Knick et al. 2003). However, sagebrush steppe communities have declined since early European settlement (Knick et al. 2003). Typically, fuels in rangelands have low horizontal continuity of the surface and canopy fuels (Keane et al. 2009; Pierson and Williams 2016). However, the fuel structure is altered due to the invasion of cheatgrass which creates a more continuous horizontal fuel structure (Whisenant 1990; Keane et al. 2009).

An increase in wildfire frequency and size across the western United States has highlighted the need to research effects of wildfire on hydrologic and erosion processes (Whisenant 1990; Monsen 1994; Keane et al. 2009; Littell et al. 2009; Miller et al. 2011; Balch et al. 2013). Wildfires impact wildlife, aquatic habitat, communities, and public safety (Pierson et al. 2001, 2011; Williams et al. 2014). The impact wildfire has on an area is determined by the degree to which burning alters vegetation, soils, inherent site characteristics, and post-fire climate (DeBano et al. 1996; Shakesby and Doerr 2006). Land managers need to know where erosion is most likely to occur following fire due to the threat post-fire erosion poses to wildfire, aquatic habitat, natural resources, and public safety (Pierson et al. 2001, 2011). In order to protect surrounding communities and natural resources post-fire, managers use various mitigation treatments to reduce the probability of erosion occurring. These mitigation treatments such as, re-seeding and applying various mulches to the soil surface are often done to reduce exposure to the soil surface and decrease erosion and runoff (Robichaud et al. 2010a).

Hydrologic response to wildfire has been well documented in forest ecosystems while few studies have focused on rangeland ecosystems (Pierson et al. 2002; Pierson and Williams 2016). There are few studies that have looked at the spatial variability of runoff and erosion following wildfire in a mountainous rangeland system. Typically, studies conducted in

rangelands are rainfall simulation studies at the hillslope scale (Pierson et al. 2011) and report increased runoff and erosion rates in the first year following fire (Pierson et al. 2002). Pierson et al. (2011) notes that the degree to which fire increase runoff and erosion is dependent to rainfall intensity, alteration of site susceptibility, and topography.

Most research has focused on the small plot scale due to the difficulties associated with the watershed scale. At the small plot scale erosion by water occurs as inter-rill erosion. Inter-rill erosion is driven by rainsplash and sheet flow (Bryan 2000; Pierson and Williams 2016). At this scale the amount of protective cover, soil characteristics, and erosive energy of rainfall determine sediment yields (Nearing et al. 2011; Nouwakpo et al. 2016; Pierson and Williams 2016). At the larger scale erosion by water is in the form of inter-rill and rill erosion processes. Rill erosion is driven by concentrated flow that forms microchannels. These microchannels form when sheet flow is concentrated by surface roughness. This concentrated sheet flow increases the flow velocity and runoff and erosion (Bryan 2000; Pierson and Williams 2016). The soil particles from inter-rill and rill erosion can be deposited on stream terraces and in vegetation and delivered to the stream channels (Ffolliott et al. 2013). The particles that are deposited into the stream can accumulate in the channel or be transported out of the watershed during precipitation events (Ffolliott et al. 2013).

Historically, post-fire erosion research has focused primarily on runoff events driven by short-duration, high-intensity thunderstorm events during summer months. Spatial patterns in soil attributes, vegetative communities, and hydrologic response within a landscape can often be described by topographic attributes calculated by Geographic Information System (GIS) software from a digital elevation model (DEM). Past studies have used terrain analysis to explain significant variables used to characterize processes on a landscape (Moore et al. 1993; Gessler et al. 1995). Analysis tools such as ArcGIS have cut costs for managers in the sense that they can use a DEM to identify, prioritize, and target management to specific regions within a landscape.

2.2. Purpose and Objectives

The purpose of this study is to improve scientific understanding of how site physical and biological attributes effect hillslope to watershed scale sediment yield and post-fire conditions on a mountainous burned sagebrush landscape.

The objectives are:

1. Quantify hillslope to watershed scale sediment yield over a two-year period (Aug 2015- Aug 2017) following wildfire.
2. Determine seasonal drivers of erosion over multiple spatial scales.
3. Develop and evaluate a conceptual model of hillslope contributions to watershed sediment yields based on measured sediment data and ecological site attributes.

2.3. Methods

2.3.1 Site Description

This study was conducted within a sub-watershed of the Reynolds Creek Experimental Watershed (RCEW) in southwestern Idaho (Figure 2.1) (Slaughter et al. 2001). RCEW is in the Owyhee Mountains, just southwest of the city of Boise and is approximately 23,900 ha in size. Precipitation in RCEW ranges from about 230 mm at northern lower elevations to > 1100 mm at higher elevations in the southern and southwestern boundary (Slaughter et al. 2001). The plant species found within RCEW are primarily those of the Great Basin Desert and alpine plant species (Stephenson 1977). The watershed is made up of volcanic and sedimentary rocks of the late tertiary age that are on top of a granitic basement of cretaceous age (Stephenson 1977). The main soil associations in RCEW are Bakeoven-Reywat-Babbington, Harmehl-Gabica-Demast, and Nannyton-Larimer-Ackmen, Dark-gray Variant (Pierson et al. 2000).

In August 2015 the Soda Fire burned roughly 112,966 ha in Owyhee (Idaho) and Malheur (Oregon) counties (USDI BLM 2015). Approximately 25% of the RCEW was burned by the Soda Fire. This study was conducted within the Murphy Creek Watershed burned in the Soda Fire within RCEW. The Murphy Creek watershed is approximately 129 ha in size and is in the upper northwestern portion of RCEW. The geology in the Murphy Creek

Watershed consists of the Salmon Creek basalt, Hoot Nanny olivine basalt, Salmon Creek basalt, and tuff associated with the upper latite unit (Seyfried et al. 2000, 2001).

The dominant soil series on the north-facing slopes are Harmehl, Demast, Rucklick, Babbington, Reywat, and Bakeoven (Figure 2.2) (Seyfried et al. 2000, 2001). All these soils generally are loams with clay loam subsoil Bt horizons at an average depth of 88 cm below the soil surface (Stephenson 1977). In contrast the predominant soils on the south-facing slopes are Harmehl, Nettelton, Reywat, Bakeoven, and Lickskillet (48 cm to bedrock) (NCSS 2010) (Figure 2.2) (Seyfried et al. 2000, 2001). These soils are well drained and generally shallow. These soils are shallow stony, gravelly, rocky, and very stony clay loams (Stephenson 1977).

The vegetation pre-fire consisted of mountain big sagebrush (*Artemisia tridentata* Nutt. Ssp. *Vaseyana* (Rydb.) Beetle.), antelope bitterbrush (*Purshia tridentata* (Pursh) DC.), common snowberry (*Symphoricarpos albus* (L.) S.F. Blake), Idaho fescue (*Festuca idahoensis* Elmer), Sandberg bluegrass (*Poa secunda* J. Presl), bluebunch wheatgrass (*Pseudoroegneria spicata* (Pursh)Á. Löve), foxtail barley (*Hordeum jubatum* L.), low sagebrush (*Artemisia arbuscula* Nutt.), rabbitbrush (*Chrysothamnus viscidiflorus* (Hook.) Nutt. Yellow rabbitbrush), bitter cherry (*Prunus emarginata* Douglas ex Hook.) D. Dietr. var. *emarginata*), and quaking aspen (*Populus tremuloides* Michx.) (Pierson et al. 2000; Seyfried et al., 2001).

Following the Soda Fire, the north-facing aspect of the Murphy Creek Watershed experienced a moderate to high burn severity. Most of the above-ground vegetation on this aspect was consumed by the fire (Figure 2.3). Post-fire the ground cover consisted of burnt plant bases, litter, ash, bare soil, and rock. The surface soils (0-5 cm depth) were hydrophobic post-fire in areas burned at high severity or where vegetation was dense pre-fire (Figure 2.4). The vegetation cover on the south-facing aspect was consumed by the fire. Areas of shrubs were shown by dark circles on the landscape mapping out the vegetation pattern. The ground cover post-fire consisted of ash, bare ground, rock, burnt litter, and burnt shrubs. Post-fire we observed considerable amounts of wind-blown sediment and organic debris into the swales

and leeward hollows in the watershed (Figure 2.5). This wind-blown material loaded these channels for several weeks after the fire.

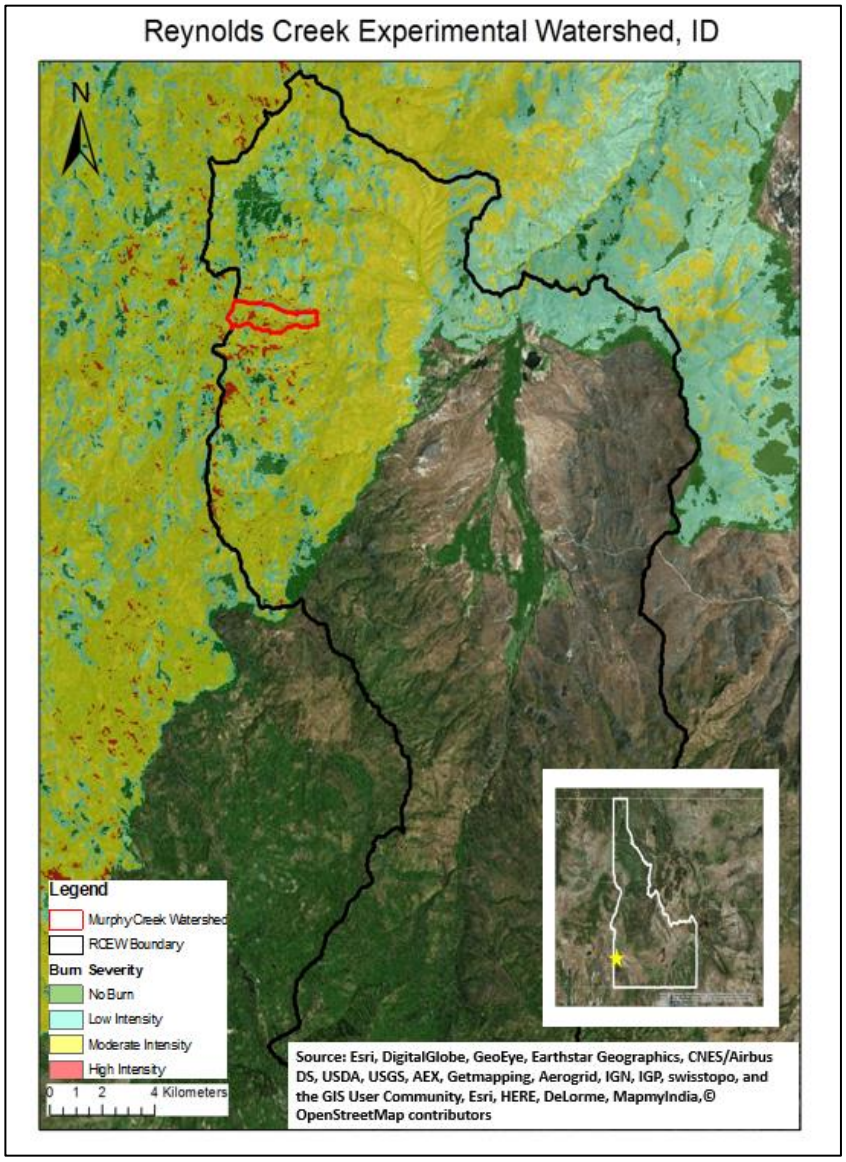

Figure 2.1. Reynolds Creek Experimental Watershed showing the study area, Murphy Creek outlined in red. Image also shows the Soda Fire burn area and severity. Data From: Esri, DigitalGlobe, GeoEye, Earthstar GeographicsCNES/Airbus DS, USDA, USGS, AEX, Getmapping,Aerogrid, IGN, IGP, swisstopo, and the GIS User Community, Esri, HERE, DeLorme, MapmyIndia, © OpenStreetMap contributors and USDA-ARS-NWRC.

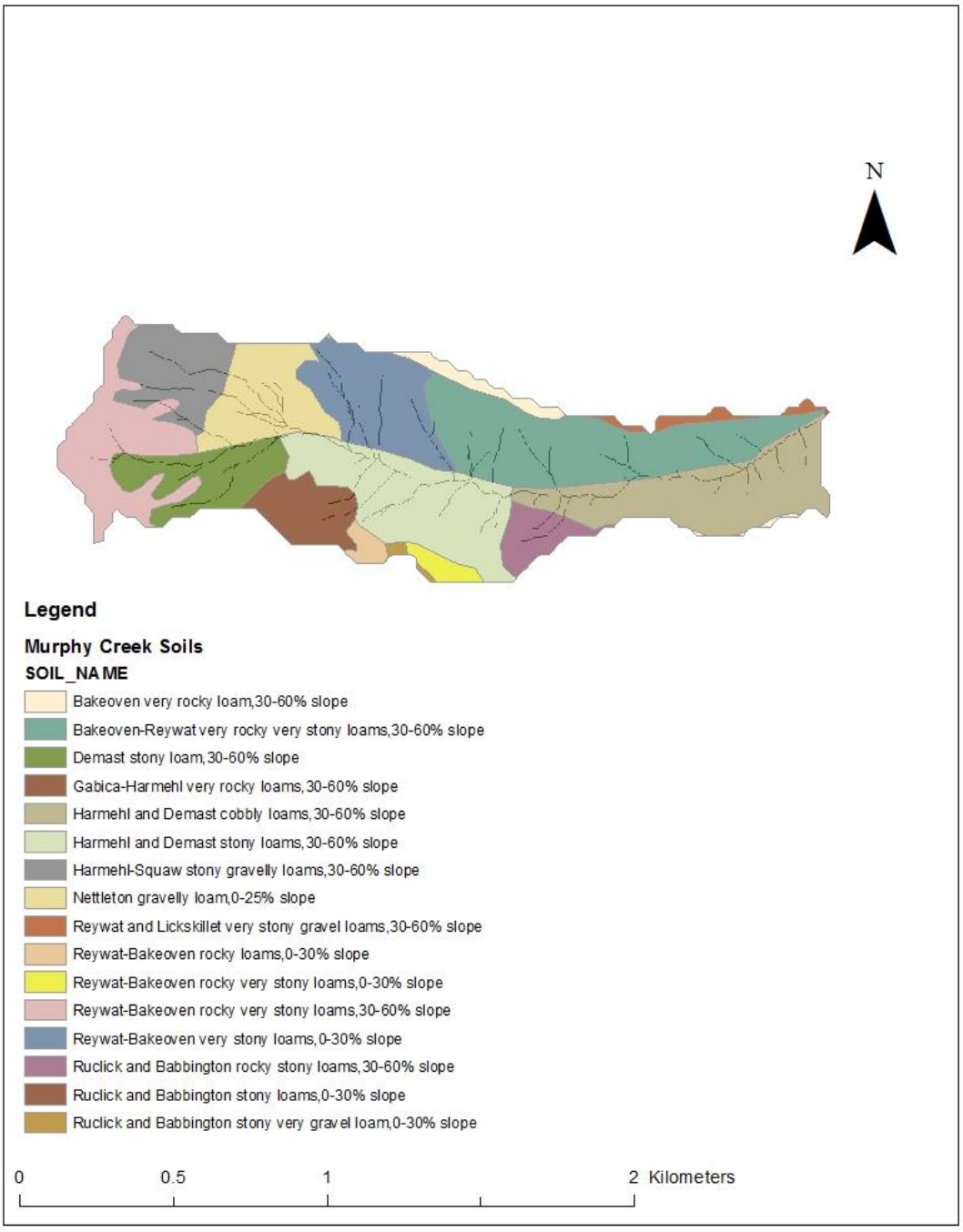

Figure 2.2. Murphy Creek watershed Soil Map. Data from: Seyfried et al. 2001.

Figure 2.3. Murphy Creek watershed following the Soda Fire. To the left is the south-facing aspect. On the south-facing aspect, the vegetation pattern is shown by the burn pattern. Shrub locations and vegetation density are shown on the south-facing aspect as the darken, burned areas. To the right is the north-facing aspect. Vegetation cover was likely much higher on this aspect and resulted in a more continuous burn and higher burn severity, as evident by the more continuous black, burned area.

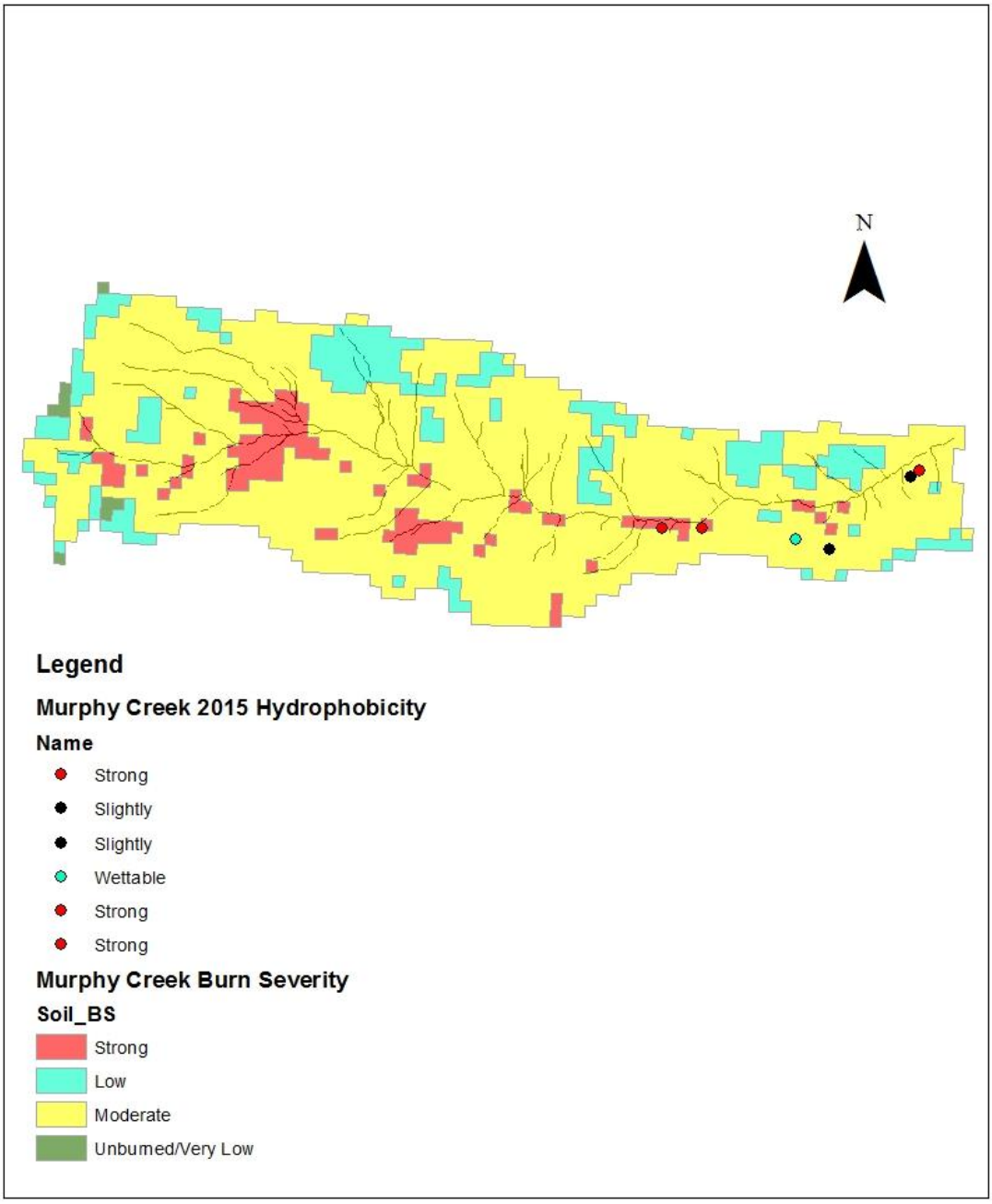

Figure 2.4. The burn severity map of the Murphy Creek watershed. The north-facing aspect burned at a high to moderate burn severity. The south-facing aspect burned at a low to moderate burn severity. However, it should be noted that the burned severity on the south-facing aspect may be higher than it actually is due to south-facing aspects in general typically having more bare ground. The hydrophobicity was strongest in areas of strong and moderate burn severity. Data from: USGS EROS (2015).

Figure 2.5. Photos of the windblown sediment and organic material observed in the side channels and leeward hollows of the watershed delivered in the weeks following the Soda Fire.

2.3.2 Overall Study Design

Streamflow data was collected using a drop-box v-notch type weir where water depth was recorded using Leopold-Steven A-35 and FW-1 strip chart recorders (Pierson et al. 2001). Data collection at the outlet of the Murphy Creek watershed dates back to 1967 as a part of the larger hydrologic study initiated at the RCEW. Streamflow measurement ceased in 1977 and was not resumed until immediately following the 2015 Soda fire. At this point two-minute average water depth of 10 second readings using a pressure transducer system was recorded by a Campbell Scientific CR1000 datalogger. A Sigma 900 automated water sampler is triggered if stage >0.1 ft and the sediment sample tubing temperature is >-0.5 °C. If stage is >0.1 ft but <0.3 ft, then a sediment sample is taken at a 48-hour interval. If stage >0.3 ft, then a sediment sample is taken at a 24-hour interval. If the change in stage >0.02 ft or greater a sediment sample is taken. If the change in stage is <-0.04 ft or less than a sediment sample is taken. In order to get the sediment concentrations from discharge the sediment samples collected by the pump sampler are taken to a laboratory for further processing. The pump samples are weighed for wet masses in the laboratory and then filtered to get the

sediment. The sediment is then dried in an oven and weighed. These methods are similar to those mentioned in Brakensiek et al. (1979).

Precipitation input into the watershed and site meteorological conditions for the study period were determined from a United States Department of Agriculture, Agricultural Research Service, Northwest Watershed Research Center (USDA-ARS-NWRC) meteorological stations Murphy Creek Watershed Station (site# 043), located at the base of the watershed, Whisky Mountain Station located within RCEW (site ID 095b) (Figure 2.6) (NWRC 2015, 2016, 2017, 2018). The meteorological stations measure hourly precipitation, temperature, relative humidity, wind, solar radiation, and soil temperature. Soil temperature data for the study period used analogous sites (Site #125 Johnston Draw and Site# 095b Whisky Mountain) (Figure 2.7) (NWRC 2015, 2016, 2017). Streamflow and sediment discharge at the watershed scale for the study period were quantified using data from the existing USDA-ARS-NWRC South Fork Murphy Creek Weir (Pierson et al. 2000; NWRC 2015, 2016, 2017, 2018).

A network of silt fences was installed and used in concert with (USDA-ARS-NWRC) watershed instrumentation to quantify hillslope- and watershed-scale post-fire erosional responses of the Murphy Creek Watershed. The impact of the wildfire on annual streamflow was examined by comparing the relationship between annual precipitation and runoff using the historic pre-fire data and post-fire data. The impact wildfire and vegetation recovery have on sediment concentrations at the outlet of the watershed was assessed by examining the changes in the sediment rating curve (log streamflow vs low sediment concentration) (Colby 1956) for the first and second year after wildfire.

The impact of wildfire on streamflow and sediment delivery was evaluated using the following approaches. The discharge and sediment concentration data from the Murphy Creek Weir has some events where sediment concentration samples were not taken. The Load Estimator a Fortran Program for Estimating Constituent Loads in Streams and Rivers (LOADEST) (Runkel et al. 2004) was used to back out annual load for the watershed both years following the fire. The overall sediment load from one year to the next was compared through the LOADEST model. Comparison of the average annual sediment concentration by

dividing the annual sediment load by the annual streamflow water volume was performed. Along with the timing of streamflow with the timing of sediment loading to the outlet of the watershed was compared to examine the importance of peak flow events on sediment loading. A historical analysis of streamflow was performed in order to compare post-fire streamflow data to long term data to determine fire effects and whether the years following wildfire in this watershed are near normal.

Missing values in the Murphy Creek meteorological record acquired from the USDA-ARS-NWRC were filled using regression methodologies to establish a full precipitation record over the study period. The Murphy Creek Meteorological Station was established in the months following the Soda Fire, resulting in missing data for the first three months of this study. Data available from one other USDA-ARS-NWRC meteorological stations (site# 095b) (NWRC 2015, 2016, 2017) at a similar elevation and with similar climate relative to the Murphy Creek Meteorological Station was acquired and used to complete the Murphy Creek precipitation and air temperature record using commonly applied regression methodologies (Ott and Longnecker 2010). A historical analysis of precipitation was performed in order to compare post-fire precipitation data to long term data to gauge if the years following wildfire in this watershed are near normal.

Figure 2.6. Image of the USDA-ARS-NWRC meteorological station, Murphy Creek (site# 043) located at the base of the watershed. The meteorological station measures hourly precipitation, temperature, relative humidity, wind, and solar radiation.

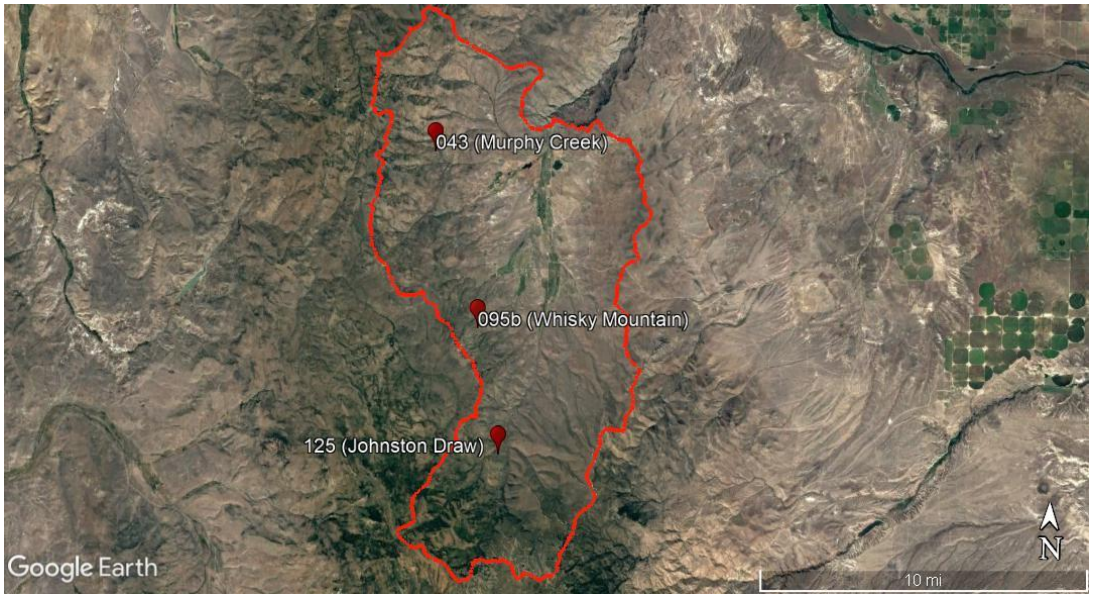

Figure 2.7. Google earth image of the research site Murphy Creek (elevation (1610m) and the two analogous watershed stations, Johnston Draw (125) and Whisky Mountain (096b) used in this study for long term and 2015 climate and soil temperature for the study period. Johnston Draw is 15.18 km south of Murphy Creek and is at an elevation of 1719 m. The Whisky Mountain station is located 8.89 km south of Murphy Creek and is at an elevation of 1533 m.

2.3.3 Silt Fence Design

Silt fences were installed throughout the Murphy Creek watershed approximately one month following the Soda fire to examine the effect of upslope topography, vegetative cover, and aspect erosion rates. An array of silt fences was installed on three different hillslopes on north and south-facing aspects (Figure 2.8). Each array consists of two small hillslope plots (11 m) bounded 10-13 m upslope by a hand-dug trench, one long hillslope plot (106 m) bounded upslope by the topographic break, and one swale plot (246 m) bounded by the upslope topography (Figure 2.9). The different plot types and sizes were installed to quantify and compare sediment delivery across spatial scales and by the different inter-rill and rill processes associated with hillslopes versus swales. Sediment for each plot type was collected in a silt fence at the base of the plot. The upslope width of the plots was defined by the natural topographic flow paths upslope of each end of the silt fence. Silt fences on short hillslope plots were 3 m wide x 2 m long. Upslope trench borders on small hillslope plots were constructed to limit upslope contributions across the width of silt fence and thereby constrain contributing areas (31-46 m^2) (Robichaud and Brown 2002). Long hillslope plots were installed with a single 5 m wide x 2 m long silt fence as the downslope base. Swale or side channel plots were installed with two silt fences as the downslope base (Figure 2.10). We anticipated more runoff would be directed through the swale plots and therefore we installed a dual fence system to contain any overflow from the uppermost fence. Silt fences for swale plots ranged from 1-5 m wide x 1-2 m long, with size dictated by swale width. All silt fences were designed and installed in a "U" shape, transverse to the slope, using methods adapted from (Robichaud and Brown 2002). For each fence installation, the ground surface to be covered by silt fence fabric was cleared of any burnt shrubs and debris. Wooden or steel fence posts were pounded into place to mark upper and lower ends of the silt fence location. Additional fence posts were driven into the ground approximately (1.2-1.8 m) apart along the downslope and side boundaries of the silt fence to frame and support to the silt fence fabric.

This study used lumite silt fence fabric (Shaw Fabric Products, Lo**v**eland, CO). The lumite fabric has a tensile strength of (79379 x 52163) grams and its permeability is 611 L m^{-2} min^{-1}(Shaw Fabric Products n.d.). The fabric was selected due to its durability, sediment trapping capabilities, and permeability (Robichaud and Brown 2002; Benavides-Solorio and

MacDonald 2005). Fabric was spread out along the fence post structure and attached to each post using roofing nails or bailing wire. Excess fabric at the base of the fence posts was routed along the ground surface (in upslope direction) and anchored into the ground using 8-gauge (203.2 mm x 50.8 mm) fabric staples. Additional pieces of fabric were overlain to cover the soil surface and excess fabric and were anchored into the ground with the fabric staples. Lastly, a trench was dug (101.6-152.4 mm) deep along the upslope end of the fence location, and a final piece of fabric was laid over the trench on the uphill side of the fence and backfilled and stapled into the trench to anchor the fabric in place (Robichaud and Brown 2002). This final piece of fabric was then pulled back over the trench onto the remaining plot surface and further anchored into the ground with fabric staples.

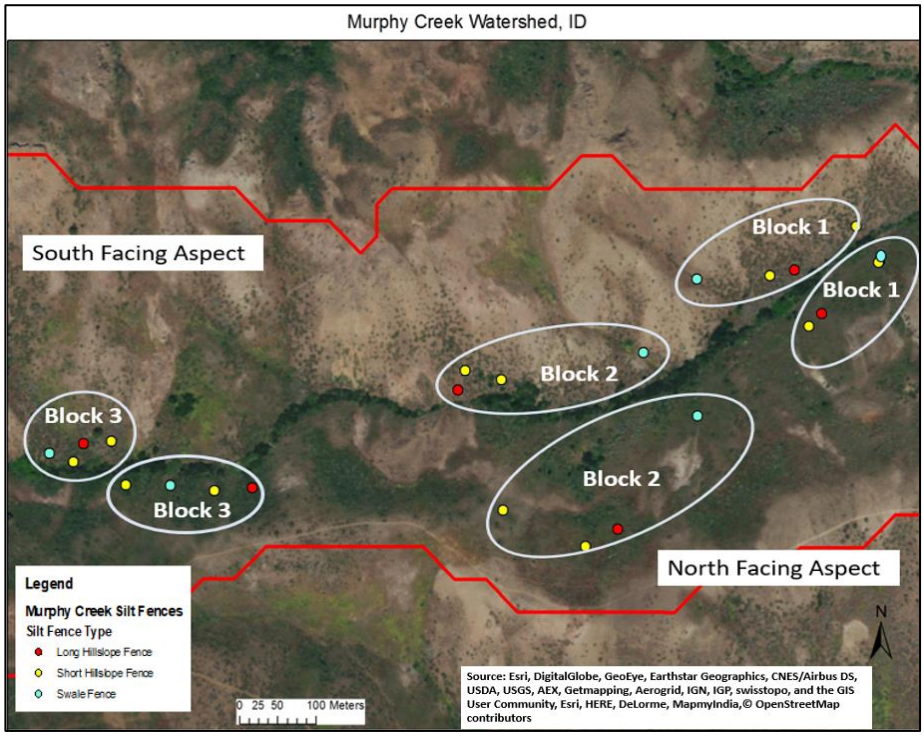

Figure 2.8. Map of the blocks in the watershed and the silt fence types. The blue dots represent swale silt fences, the red dots represent long hillslope silt fences, and the yellow represents the short hillslope silt fences. Data Source: Esri, DigitalGlobe, GeoEye, Earthstar Geographics, CNES/Airbus DS, USDA, USGS, AEX, Getmapping, Aerogrid, IGN, IGP, swisstopo, and the GIS User Community, Esri, HERE, DeLorme, MapmyIndia, © OpenStreetMap contributors.

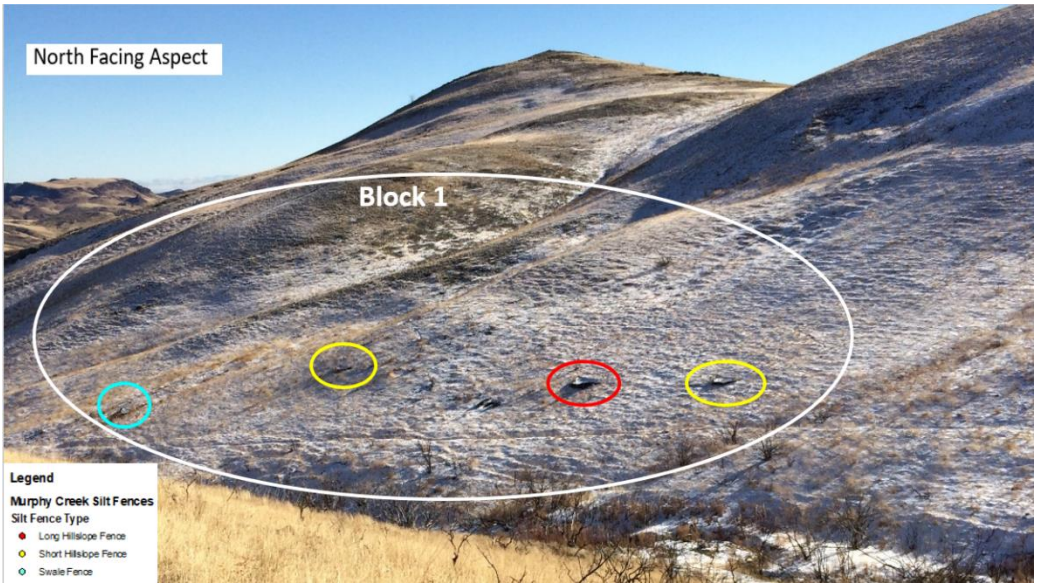

Figure 2.9. A photo of the silt fence array in a block and the upslope contributing areas.

Figure 2.10. Image of a swale plot showing how the two silt fences are placed as the downslope base.

Trips to the Murphy Creek watershed were made all year to check the fences and sediment delivery. Silt fences were cleaned out seasonally as needed to measure the sediment

delivered from hillslopes and swales. Sediment within fences was quantified at each clean out by bucket weighing all removed sediment on site (Robichaud and Brown 2002). While cleaning out fences, we looked to see if the material appeared to be homogenous throughout. In cases with obvious heterogeneous sediment patches (e.g., windblown, coarse sediment, fine sediment, etc.), each different patch was sampled separately. A sub-sample (1 L bottle or 348 cm^3 soil can) was taken with every bucket weighed unless the sediment appeared to have the same texture, moisture content, and organic matter in which case every other bucket was sub-sampled. Sub-samples were taken to determine water and soil masses of respective bucket sample sediment. The sample bottles and soil cans were tightly capped in the field and taken to laboratory for further processing. The samples were weighed for wet mass in the laboratory, then dried in an oven at 55 °C to a stable dry mass and reweighed. The total mass of water in each bottle and soil can was then determined as the difference of the wet and dry masses and the quantified water and sediment percentages for the respective sample were used to determine the water and sediment masses for the associated field bucket sample. A particle size distribution of plot-sampled sediment for each silt fence was assessed through sub sampling of the total sediment load captured the respective fence. To create a representative soil sample of material captured in each silt fence the sediment from all bottles and soil cans associated with each respective fence were mixed together until homogenous and then were sub-sampled for analysis.

2.3.4 Vegetation Measurements

Vegetation was measured in order to assess vegetation recovery and impact on erosion rates following the fire. Within each block of silt fences, two characterization plots (4 m long x 2 m wide) were installed to quantify canopy and ground cover, ground surface roughness, and soil water repellency at the small hillslope plot scale. Plot locations were marked for subsequent year sampling by pounding t-posts into the ground at the upslope and downslope ends of each plot (Figure 2.11). For each plot, canopy and ground cover were measured using the line-point intercept method (Herrick et al. 2005). Canopy and ground cover by life form were recorded for 20 points (20 cm spacing), along each of nine transects, spaced 20 cm apart and oriented perpendicular to the hillslope profile (180 points per plot). Percent cover by cover type for each plot was determined from the number of point contacts or hits for each

respective life form divided by the total number of point's sampled (Pierson et al. 2010). The plot ground surface roughness was measured as the average of standard deviations of ground surface heights measured across the line-point transects (Pierson et al. 2010). The relative ground surface height at each sample point was derived as height of a survey transit level line above the respective sample point.

Vegetation canopy and ground cover for each long hillslope and swale plot were quantified using line-point intercept methods (Herrick et al. 2005) along four 30 m transects. Transect locations for each hillslope and swale plot were determined by dividing the upslope distance from the respective silt fence to the top of the hillslope topographic break into four evenly spaced sections. A single transect was established spanning in each section, oriented parallel to the hillslope contour (Figure 2.11). These transects were installed and sampled to capture the variability in cover from the base of each swale and long hillslope plot to the top of the hillslope. Canopy and ground cover by lifeform were measured at 0.5 m increments along each 30 m transect (61 points per transect). Percent cover by cover type for each transect was determined from the number of point contacts or hits for each respective life form divided by the total number of points sampled (Pierson et al. 2010). Percent cover by cover type for each hillslope and swale plot was determined as the average of respective measures across each of the four transects in the plot.

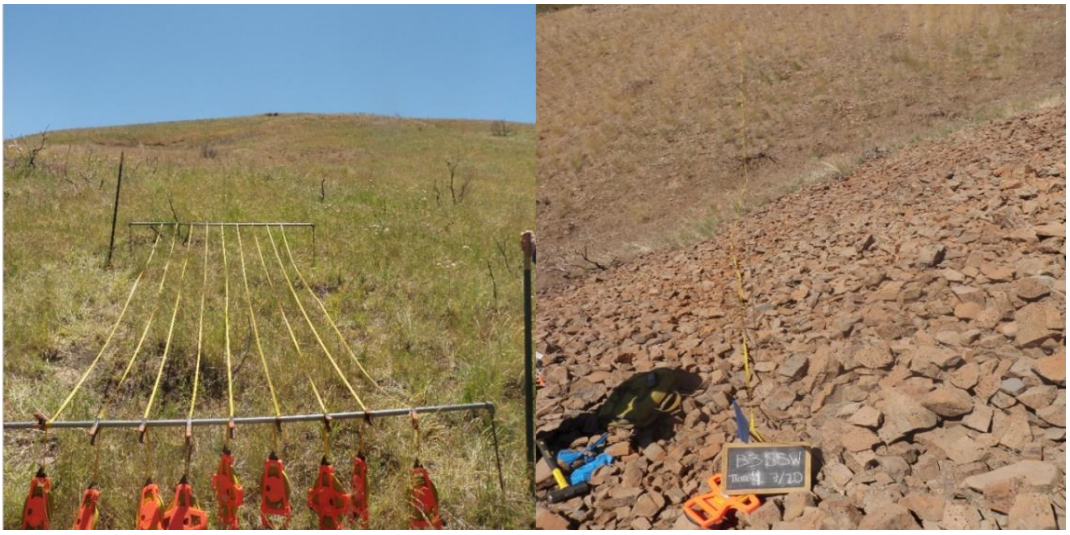

Figure 2.11. Image of the two different scales of vegetation measurements taken in Murphy Creek. Left photo is the small vegetation plots. The photo on the right is an image of a vegetation transect.

2.3.5 Water Repellency Measurements

Water repellency measurements were performed to determine where and when hydrophobicity was strongest in the years following the fire. Water repellency at 0-5 cm depth was measured within each characterization plot along one of the 4m vegetation transects. A single transect was randomly selected within each site characterization plot and was sampled for soil water repellency at 40 cm increments downslope (11 points) using the Water Drop Penetration Time (WDPT) procedure (DeBano 1981). At each sampling point, three water drops were placed on the mineral soil surface and the time required for each water drop to infiltrate was recorded (up to a maximum of 300 s). Following this procedure 1 cm of soil was excavated and the procedure was repeated with three more drops. WDPT sampling iterations continued to a soil depth of 5 cm. Mean soil water repellency at each 1-cm depth (0-, 1-, 2-, 3-, 4-, and 5-cm depths) for each plot was determined as the mean of the three WDPT (s) samples for the respective depth. The mean soil water repellency across all sampled soil depths on each plot was derived as the average of the respective WDPT means for 0-, 1-, 2-, 3-, 4- and 5-cm soil depths. Soils were classified as wettable when WDPT was less than 5 s,

slightly water repellent when WDPT ranged from 5 to 60 s, and strongly water repellent when WDPT was greater than 60 s (Bisdom et al. 1993).

2.3.6 Sediment Yields and Spatial Patterns

In order to examine the key factors driving the spatial variability post-fire soil erosion we conducted a correlation analysis between observed total sediment yield and erosion rates to observed and predicted vegetation and topographic attributes calculated from a 3m spatial resolution DEM. The attributes tested in this study were found using a DEM (3 m spatial resolution) from 2007 (Glenn 2007) and SAGA GIS. The characteristics derived are as follows: slope steepness, solar insolation (Wilson and Gallant 2000), wetness index (Moore et al.1993; Böhner and Selige 2006), stream power index (Moore et al. 1991,1993), LS factor (Moore et al. 1991), aspect (Moore et al. 1991), relative slope position (Böhner and Selige 2006), curvature index (Moore et al. 1993), depth to the valley, vertical distance to valley, wind effect, and flow accumulation (Bolstad 2012). The average, minimum, and maximum topographic characteristic found within the upslope contributing area to each silt fence was calculated using the zonal statistics tool in ArcGIS. The contributing areas to each silt fence was delineated using the D8 flow routing routines in ARC GIS with a DEM developed in 2014 (3m spatial resolution) (Ilangakoon et al. 2016). Methods for this analysis were adapted from Cooley (2016).

In this study we define erodibility as the slope of the sediment rating curve relationship (i.e. log streamflow vs log sediment concentration) (Colby 1956). The term erosion rate is used when referring to the tonnes of sediment delivered per unit contributing area (i.e. t/ha) and sediment yield is used when referring to total sediment delivered to an outlet point over a particular time period (tonnes/yr).

Since this analysis included areas of the watershed where vegetation cover and electrical conductivity (EC) were not measured the random forest algorithm in the R software package was used to create a vegetation layer based on the observed vegetative characterization data. This included the percentage of canopy and ground cover life forms were reported for the small-scale vegetation plots. Percentage for each life form for canopy and ground cover was reported every 6m on each 30m transects in the larger vegetation plots

(long hillslope and swale). The primarily spatial input data to the random forest model was the topographic attributes calculated from the 3 m spatial resolution DEM and 2015 NAIP imagery (USDA-FSA-APFO 2016a, 2016b).

The degree to which the derived spatial topographic attributes and vegetative maps explained the spatial variability in soil erosion was assessed based on a Pearson correlation analysis. The correlation analysis was performed between the measured erosion and the topographic, soil, and vegetation cover characteristics for each of the different plot types and delivered sediment to the silt fences.

A soil erosion risk map was created for the entire Murphy Creek basin using the most highly correlated attributes as a guide. The watershed was delineated into primary hillslopes and swales contributing to Murphy Creek. Each swale or hillslope was classified as high, moderate, or low erosion risk based on the first-year erosion rates.

2.4. Statistical Analysis

The determination of statistical significance was evaluated using SAS software, version 9.4 (SAS Institute Inc. 2013). Statistical analyses of silt fence sediment values and canopy and ground cover variables were conducted using a mixed model approach in SAS (Littell et al. 2006). Mean separation analyses were restricted to 1) by plot-type within aspect between years and 2) by plot-type within-year across aspects. Between-years comparisons by plot-type for a given aspect (north or south) applied a mixed model with two treatments, Year 1 and Year 2. Within-year comparisons by plot-type across aspects applied a mixed model with two treatments, north aspect and south aspect. Normality of silt fence sediment values and vegetation cover data was tested prior to ANOVA using the Shapiro-Wilk test and deviance from normality was addressed by data transformation. Back transformed means are reported. Mean separation was determined using the LSMEANS procedure (SAS Institute Inc. 2013). All reported significant effects were tested at the $P<0.05$ level.

2.5. Results

2.5.1 Hydrologic Response

The total precipitation recorded in the first two years after the wildfire were considerably different. The total precipitation recorded in the first-year post-fire (2016 water year) was 473 mm, 19 mm above normal (454 mm). Whereas, the total annual precipitation for the second-year post-fire (2017 water year) was 649 mm, 195 mm above normal (454 mm).

2.5.1.1 Watershed Scale Streamflow and Sediment Yield

Similar to the trend in precipitation the streamflow during the second year was much greater than that observed in the first year after fire. The annual water yield during the second-year post-fire (304 mm) was more than double (i.e. 111% greater) in magnitude than the water yield observed during the first-year post-fire (144 mm). As seen in Figure 2.12, there exists a strong relationship between annual precipitation and annual water yield from the Murphy Creek watershed. The observed post-fire 2016 and 2017 water yield closely followed the historic unburned relationship with annual precipitation. Much of the streamflow in the second year occurred during a large snowmelt event. The timing and magnitude of streamflow the first year following the fire was roughly similar to long-term Murphy Creek streamflow data collected before the fire (1968-1977) (Figure 2.13). Whereas, with the exception of 1972 water year, the observed streamflow during the second year was one of the highest on record (Figure 2.13).

Analysis of the observed streamflow and sediment concentration data collected at the outlet of the Murphy Creek watershed indicated that wildfire greatly increased sediment transport the first-year post-fire at the watershed outlet (Figure 2.14). The total sediment load collected at the watershed outlet between January 1, 2016 and September 30th, 2016 was 318 tonnes (2.5 t ha^{-1}) based on observed sediment concentration and streamflow using the LOADEST model (Figure 2.14). This total does not represent a complete water year as it does not include any sediment delivered between October and December 2015 since the water sampler wasn't installed until the beginning of January 2016. Based on the observed streamflow and sediment load the average sediment concentration during this period was

1,712 mg/liter in the first year following the fire. The total sediment load delivered during the second year was very similar to the amount of sediment delivered during the first year. In the second year following the fire the sediment yield increased from 318 tonnes to 393 tonnes (Figure 2.15). During this second year the total amount of streamflow leaving the watershed was more than double the first year but in terms of sediment load there was not much difference between the two years. In the second-year post-fire the watershed erosion rate increased to 3.0 t ha^{-1}. In the second year the average annual sediment concentration was 1,000 mg/liter. During the first year there were two large peaks in streamflow in January and February. During these events the watershed was experiencing freezing conditions with rain on snow and frozen soil which contributed to sediment delivery to the silt fences and likely these pulses of high sediment concentration collected at the outlet. During the second-year streamflow was highest during February 8th and 9th. The vast majority of the annual total sediment load (99%) at the watershed outlet during the second year occurred during this warm snowmelt event. Based on changes in the observed slope of the sediment rating curve the average erodibility for the watershed was much greater in the first-year post-fire than in the second year (Figure 2.16).

2.5.1.2 Hillslope Scale Variability Erosion Rates

The greatest sediment delivery to the silt fences occurred during the fall (September-November) and winter (December-February) months the first-year following the fire. In the fall months immediately following the Soda fire the watershed received 139 mm of total precipitation (29% of the annual total) and 179mm of total precipitation (38% of the annual total) in the fall and winter months. In general, small-scale plots (short hillslope plots) relative to the long hillslope plots and swales had the greatest erosion rates (Figure 2.17). These small-scale plots also had the highest spatial variability with some plots receiving very little to no measurable sediment. The average annual erosion rates from the small-scale plots was 4.8 t ha^{-1}. In particular, the small-scale plots located on the north-facing slopes had the highest erosion rates, averaging 8.6 t ha^{-1}, and had the greatest spatial variability. For example, in block two on the north-facing slope the erosion rates of the small-scale plots were 0.3 t ha^{-1} and 17.2 t ha^{-1} in the first year following the fire (Table 2.1). These small-scale plots are

located within the same block and aspect, yet the total sediment delivered from these areas is greatly different. This spatial variability was observed in each block on both aspects.

The large-scale plots (long hillslope plots and swales) had lower mean erosion rates compared to the small-scale plots in the first year following the fire. All the silt fences on the north-facing aspect received sediment the first year following the fire whereas, only 50% of the south facing silt fences received sediment (Figure 2.17). In the weeks following the fire we observed considerable amounts of sediment and organic material loading the side channels, swales and leeward hollows as deposits of wind blown sediment. In terms of overall sediment load from the hillslope regions, the swales collected the most sediment. The swales had a mean erosion rate of 0.5 t ha^{-1} in the first year following the fire. The north-facing swales had a higher mean erosion rate of 0.7 t ha^{-1} than the south-facing swales 0.2 t ha^{-1} in the first-year post-fire (Figure 2.18) (Table 2.1). There was not a significant difference in erosion rates between the north-facing swales and the south-facing swales in the first-year post-fire; however, the erosion rates in the swales on the south-facing aspect had higher spatial variability than the swales on the north-facing slope (Figure 2.19). The majority of the sediment collected in the swales on the south-facing slope, 62%, was collected in one of the swales, B3SSW. The primary source of sediment within this swale was a single head cut located downstream of a spring (Figure 2.20). Very little noticeable rilling occurred elsewhere within the upslope contributing area to the swale. The mean erosion rates from the long hillslope plots (0.8 t ha^{-1}) were larger than the swales yet less than the small-scale plots the first-year post-fire. Similar to the trends observed with the swale and small-scale plots the large-scale plots located on the north-facing slopes collected more sediment than the plots located on the south-facing slopes (Table 2.1).

The sediment delivery to the silt fences in the first-year post-fire mainly occurred in the fall and winter months. In October there were two major events with several smaller rain events wetting the soil in Murphy Creek (Figure 2.21). In the month of November, the watershed experienced freezing and thawing conditions (Figure 2.21 and 2.22). In similar watersheds located 8.9 km and 15.2 km south of Murphy Creek watershed at similar elevations, 1533 m and 1719 m, (site #125 Johnston Draw and site # 095b Whisky Mountain) (NWRC 2015, 2016), in RCEW the north-facing aspect was frozen on November 19th with

warming occurring around November 24th and back down to freezing temperatures November 30th until early December. During this period of freezing and thawing, sediment was delivered to five of the 30 silt fences. Trips to the watershed were made during this time to check on the sediment delivery to each fence. The soils were frozen in the watershed during a November 30th site visit (Figure 2.23) and it is likely that November 19th storm was a rain on frozen soil event. Soil temperature data suggest that both the January 29th and February 14th storms was influenced by frozen soil on the north-facing slopes. The data suggest that the south-facing slope was not frozen during the large February 14th storm. (Figure 2.21 and 2.22). Sediment was actively moved to the silt fences during these large winter storms. However, no sediment delivery to the silt fences occurred during 28 mm of rainfall that fell on the watershed during the summer months (June-August).

Similar to the first year, year two sediment delivery to the silt fences only occurred during the winter months. The watershed received 46% (301 mm) of the total annual precipitation during these winter months. Sediment delivery mainly occurred in the swales with minimal sediment delivery from the short hillslope and long hillslope plots. Only 42% of all the silt fences in the watershed received sediment in the second-year post-fire. The majority (60%) of the silt fences located in the swales had measurable sediment during the second year after wildfire (Figure 2.24). Similar to the first year, all swale silt fences captured some sediment however the mean observed erosion rates above the swales was larger on the north-facing slopes (0.6 t ha^{-1}) than the south facing slopes (0.2 t ha^{-1}) (Figure 2.18 and 2.19). Like the first year, over 90% of sediment collected on the south facing slope was captured by the swale having the upslope head cut, B3SSW. As a result, there was not a statistically significant difference in erosion rate between the north-facing swales and south-facing swales in the second-year post-fire.

As with the first year following the fire, the erosion rates in the second-year post-fire were mainly driven by winter events occurring in January and February. The largest streamflow event over the two-year monitoring period which took place on February 7th-9th 2017 was due to warm snowmelt period initiated by rain on snow (Figure 2.22 and 2.25). The majority of the sediment transport to the watershed outlet and the silt fences took place during

this event. Despite the watershed receiving and additional 269 mm of precipitation in the spring and summer no sediment transport to the silt fences was observed after this event.

The greatest reduction in sediment delivery after the first-year post-fire occurred at the small-scale with the short hillslopes (Figure 2.17 and 2.24). The short hillslope plots mean erosion rates on both aspects declined in the second-year post-fire (north-facing aspect 0.04 t ha^{-1}, south-facing aspect 0.1 t ha^{-1}). The erosion rate from the most erosive south-facing short hillslope silt fence declined by 81%. Although there was no change in which silt fences received sediment delivery, there was a decline in the amount of sediment delivered. In contrast to the small-scale plots, the erosion rates from the large-scale plots were relatively consistent in both of the years. The swales consistently had erosion on the north-facing aspect and other than the swale with the head cut, B3SSW, the south-facing slopes consistently had low erosion rates.

At the watershed scale the erosion rates were also similar during both years. Figure 2.26 captures the change in erosion rates with scale and time throughout the watershed. As seen in the figure, erosion rates declined with scale the first year after fire and increased with spatial scale the second year after fire. This temporal difference was largely due to the dramatic drop in erosion rates in the small scale plots the second year after wildfire. Although there is a trend towards higher erosion rates with increasing bare soil cover, there is wide variability across the site (Figure 2.27).

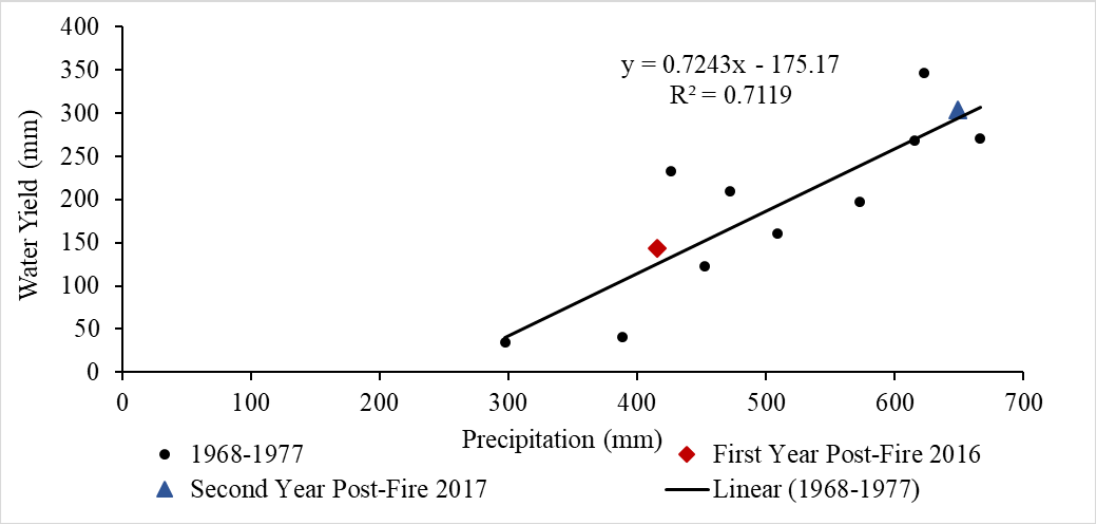

Figure 2.12. Water yields and precipitation for long term data and the first and second year following the fire. The first and second years post-fire were similar to the long-term data suggesting that these years were likely near normal.

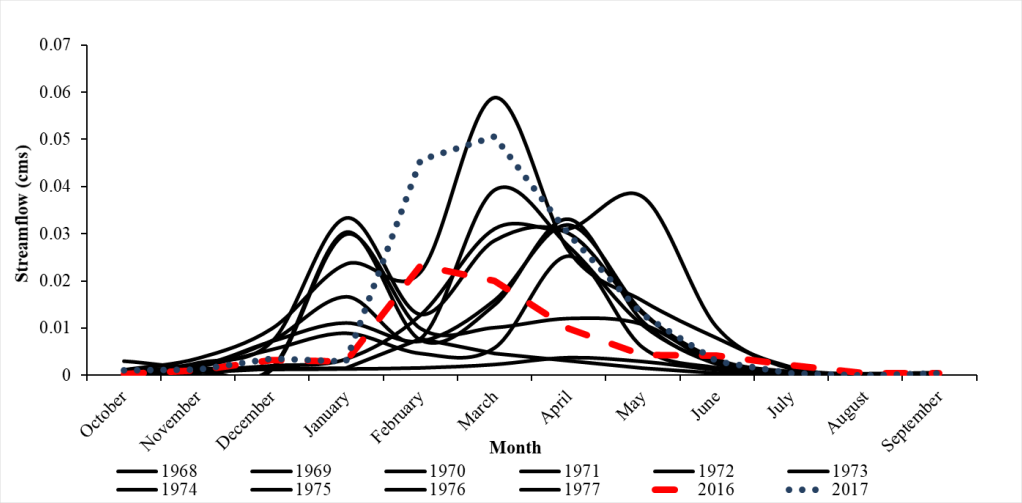

Figure 2.13. This figure is showing the long-term Murphy Creek watershed streamflow data from (1968-1977) water years. The long-term data is represented by the black solid lines. The streamflow one-year post-fire (2016 water year) is represented by the dashed red line and the second-year post-fire (2017 water year) shown as dotted blue line. The first-year post-fire streamflow was not abnormal compared to the long-term data. The second-year post-fire streamflow was higher than the majority of the long-term data however there was one year, 1972, that was higher.

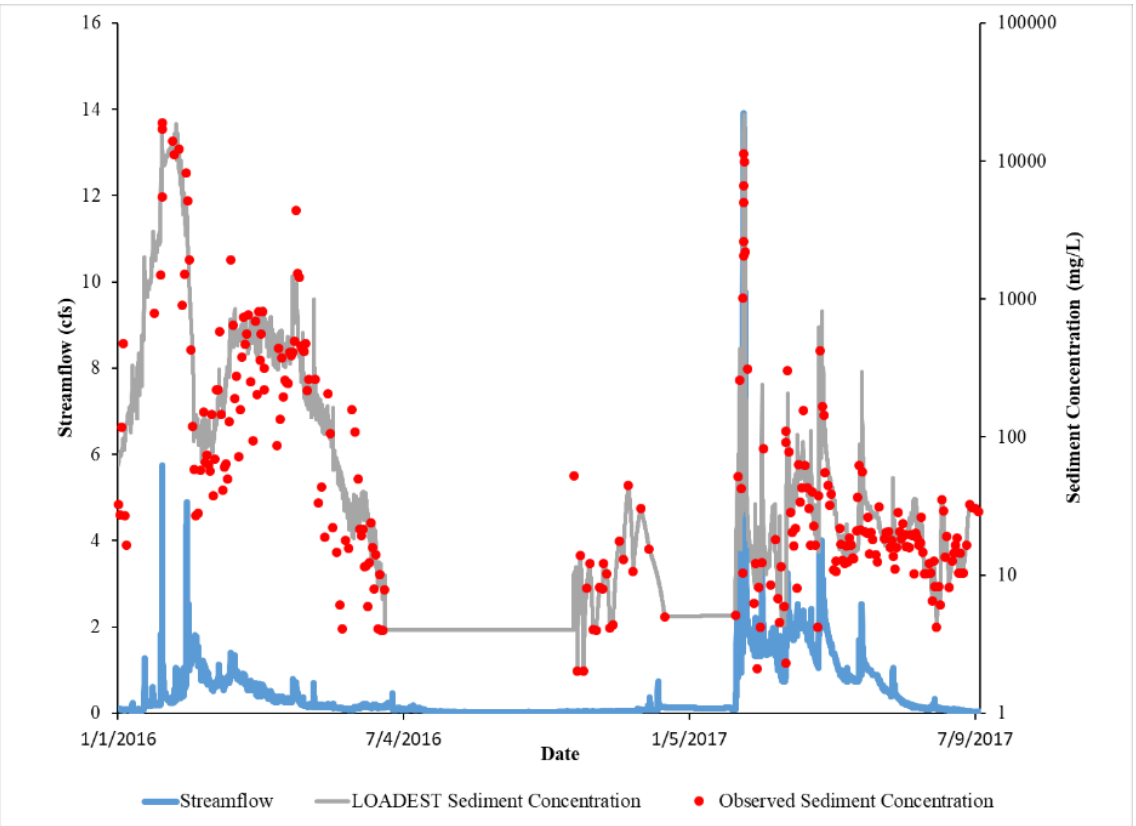

Figure 2.14. The measured streamflow and observed sediment concentration data shown with the LOADEST sediment concentration data shown in gray represents how the data was fit using LOADEST.

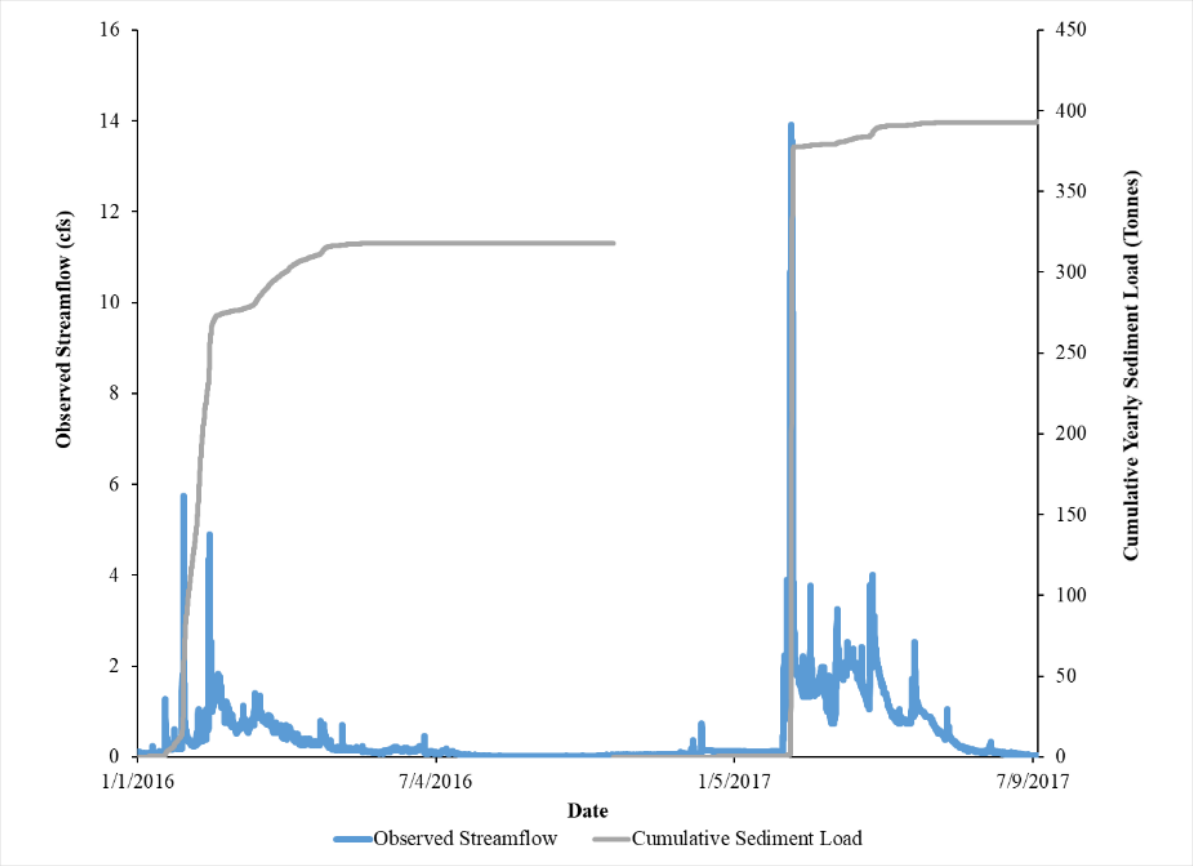

Figure 2.15. This figure is showing the observed streamflow measured at the Murphy Creek watershed for the study period and the cumulative yearly sediment load in tonnes. In the first year following the fire the cumulative sediment load was 318 tonnes. In the second year following the fire the cumulative sediment load increased to 393 tonnes.

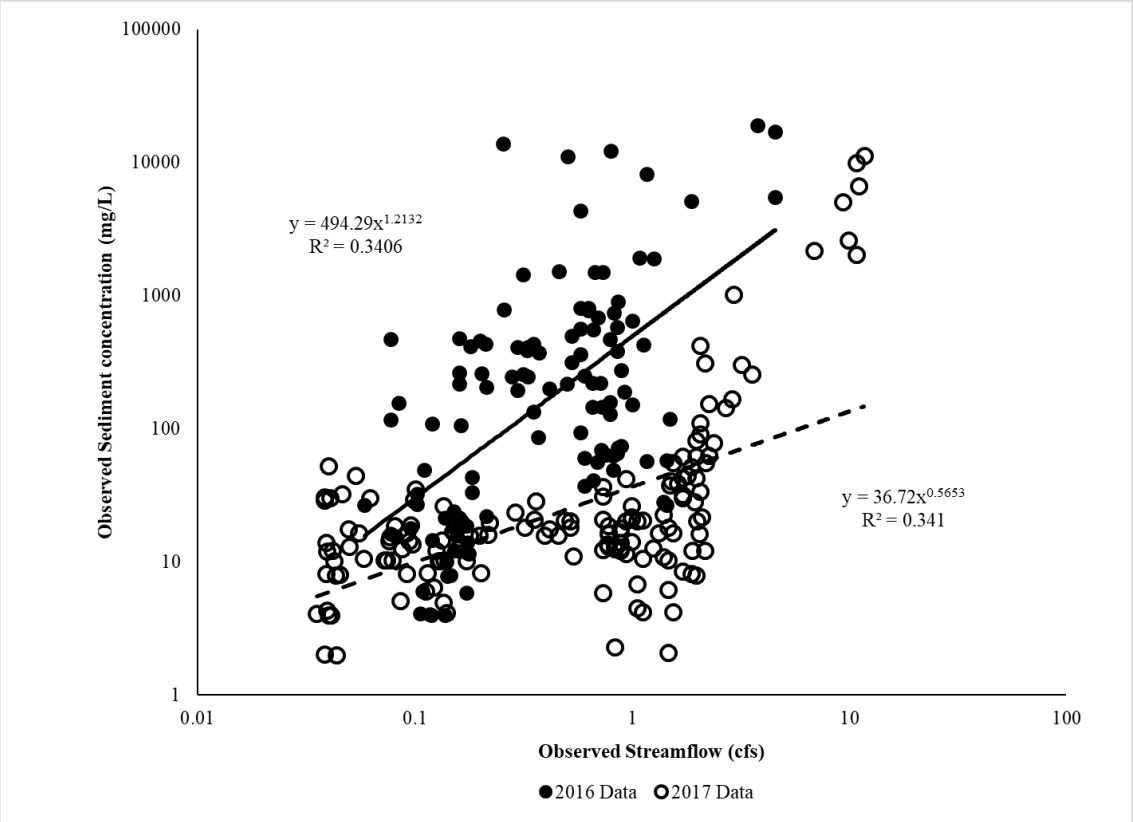

Figure 2.16. The relationship between streamflow and the sediment concentrations in the first year following the fire (2016) and the second year following the fire (2017). In the first-year post-fire erodibility was higher as indicated by the steeper slope shown with the solid line. In the second year-post-fire erodibility was lower as indicated by the dashed line.

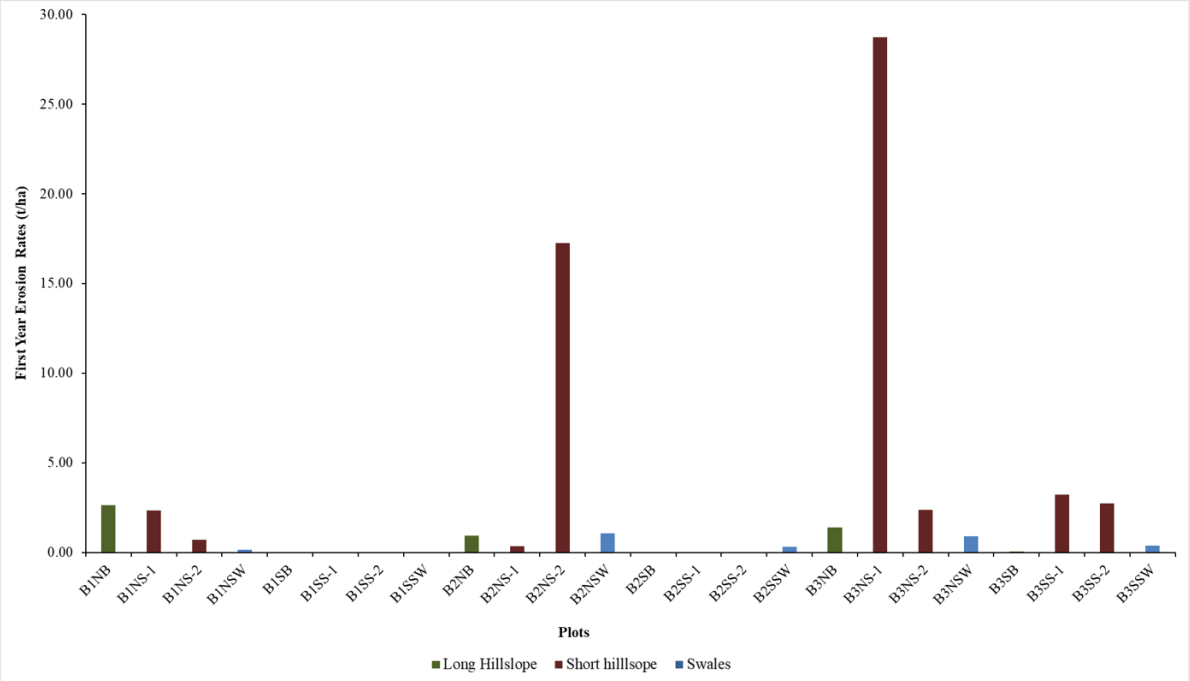

Figure 2.17. Graph showing the first-year erosion rates for each of the silt fences in the Murphy Creek watershed. The small-scale plots (short hillslope plots) received higher erosion rates than the large-scale plots (Long hillslope and swale) in the first-year post-fire. The north-facing silt fences had the most fences with sediment delivery.

Table 2.1. Table of the erosion rates for each plot type on both aspects.

Murphy Creek Watershed Erosion Rates (t/ha)				
	North-Facing Aspect		South-Facing Aspect	
Plot type	2016	2017	2016	2017
Short Hillslope	0.3-28.7	0.0-0.2	0.0-3.2	0.0-0.6
Long Hillslope	0.9-2.6	0.0-0.1	0.0-0.1	0.0-0.05
Swale	0.1-1.1	0.3-0.9	0.01-0.4	0.01-0.6

Figure 2.18. The north-facing swales in year one and two post-fire. The north-facing swales produced the highest erosion rates both years following the fire and are the most susceptible to erosion.

Figure 2.19. The south-facing swales in year one and two post-fire. The south-facing swales produced lower erosion rates than the north-facing swales both years following the fire. In the first year only two of the three swales had high sediment delivery with one having the most. The third swale produced the highest erosion rates both years post-fire due to the head cut.

Figure 2.20. A close-up image of the head cut above the swale in block three, B3SSW, on the south-facing aspect.

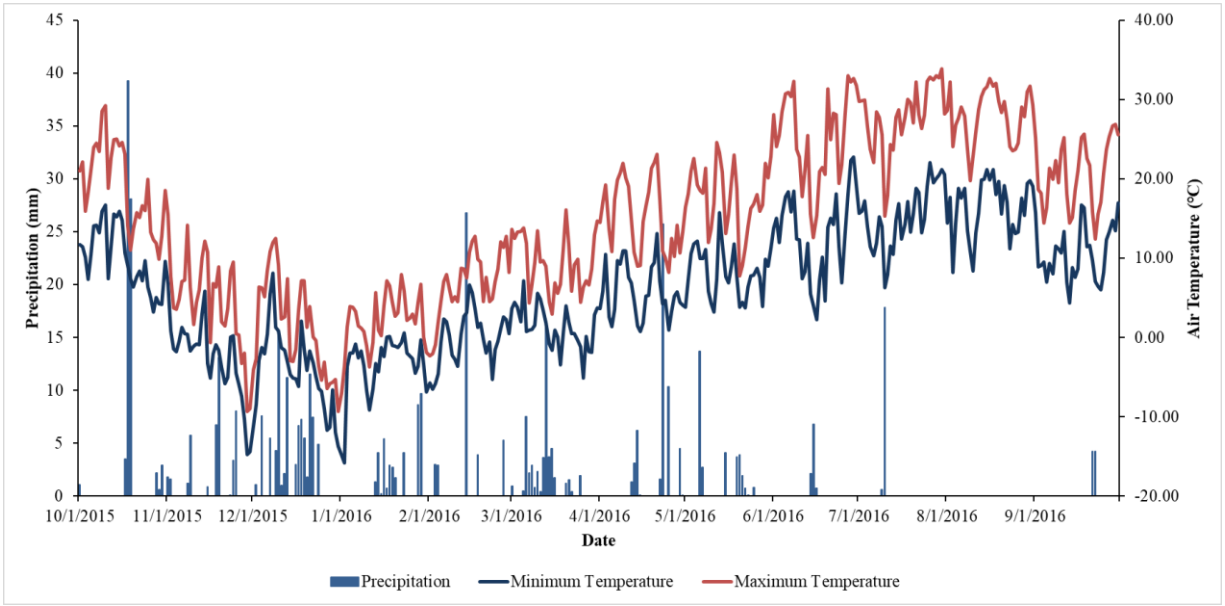

Figure 2.21. Murphy Creek watershed 2016 water year precipitation and air temperature.

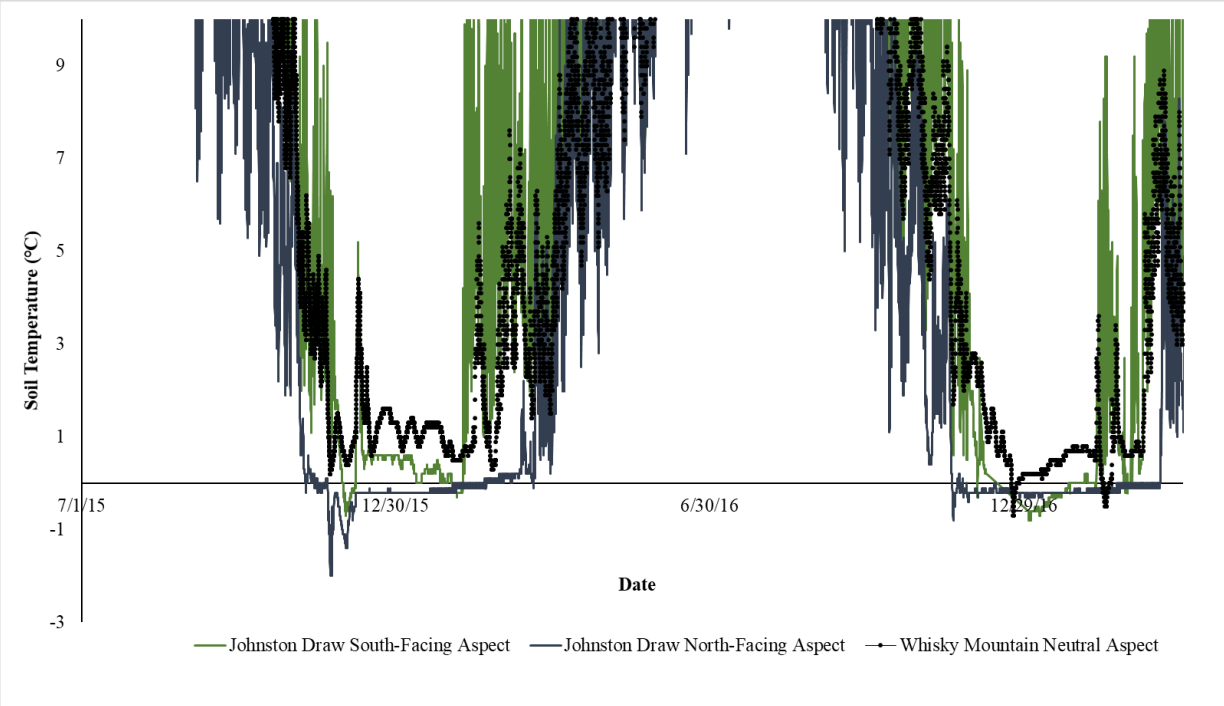

Figure 2.22. Johnston Draw and Whisky Mountain sites soil temperature. The Johnston Draw site was chosen due to soil temperature data on each aspect for the study period. The Whisky Mountain site was used due to similar elevation as Murphy Creek and it being a neutral aspect in order to compare. This figure is highlighting soil freezing and thawing during sediment delivery winter periods both years following the fire.

Figure 2.23 The Murphy Creek Watershed in the winter months following the fire in 2015. Freezing and thawing of the soil occurred during the month of November around the 30th. This photo was taken on November 30th, 2015.

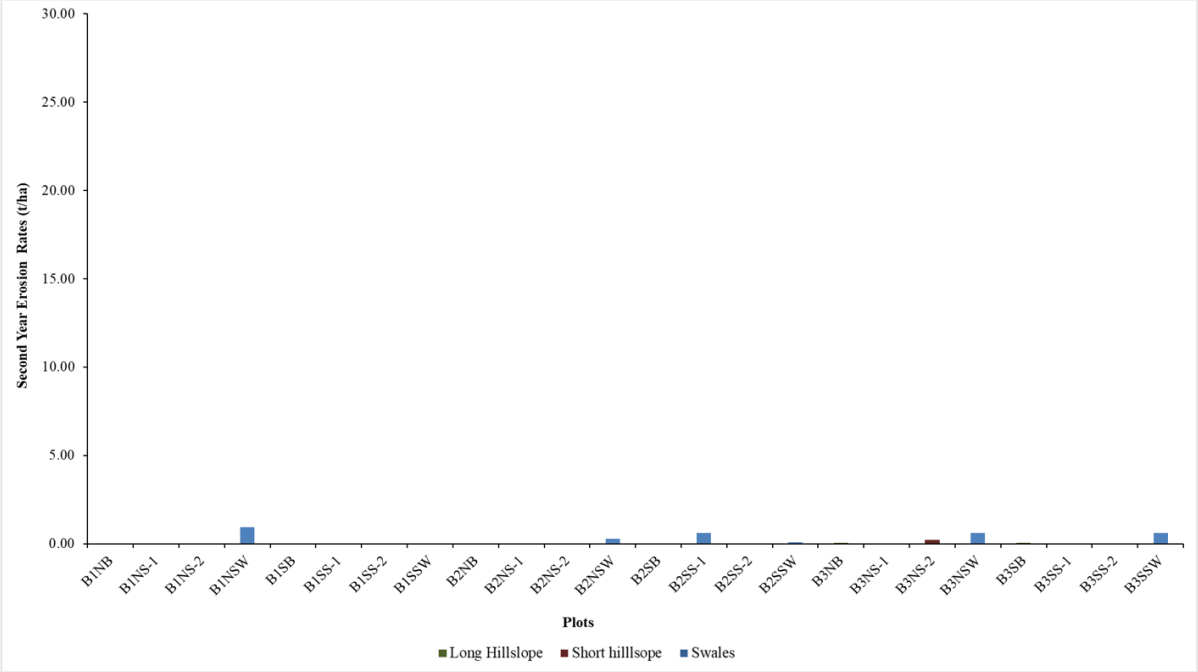

Figure 2.24. Graph showing the second-year erosion rates for each of the silt fences in the Murphy Creek watershed. The sediment delivery was mainly to the swales in year two. The erosion rates were higher in year one and the amount of silt fences with sediment declined drastically in the second-year post-fire.

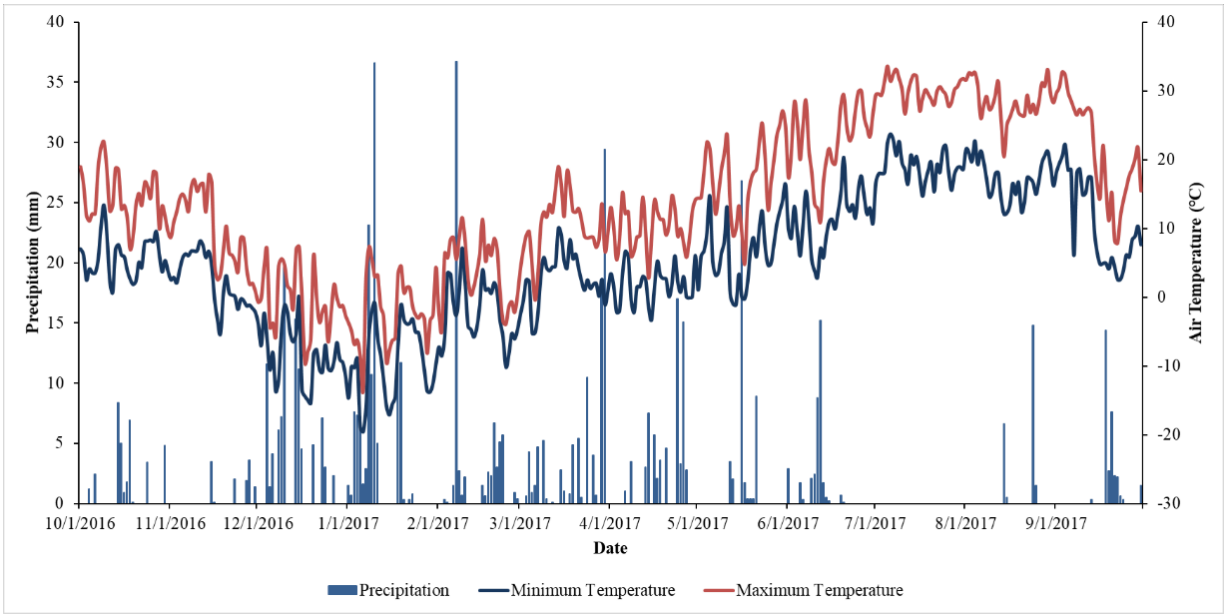

Figure 2.25. Murphy Creek watershed 2017 water year precipitation and air temperature.

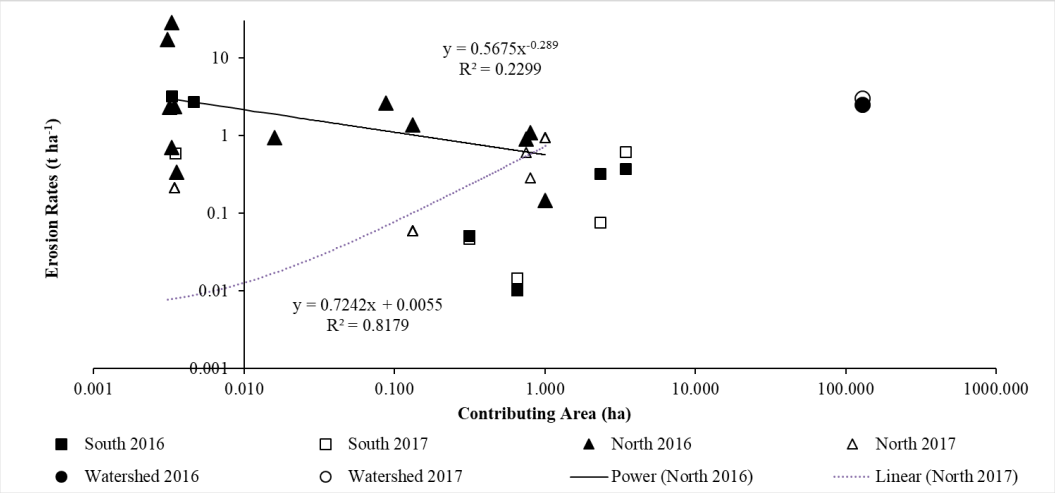

Figure 2.26. Erosion rates of the small-scale plots (short hillslope plots) and the large-scale plots (long hillslope plots and swale), and watershed are compared with the contributing area (ha). Only the silt fences with sediment are shown.

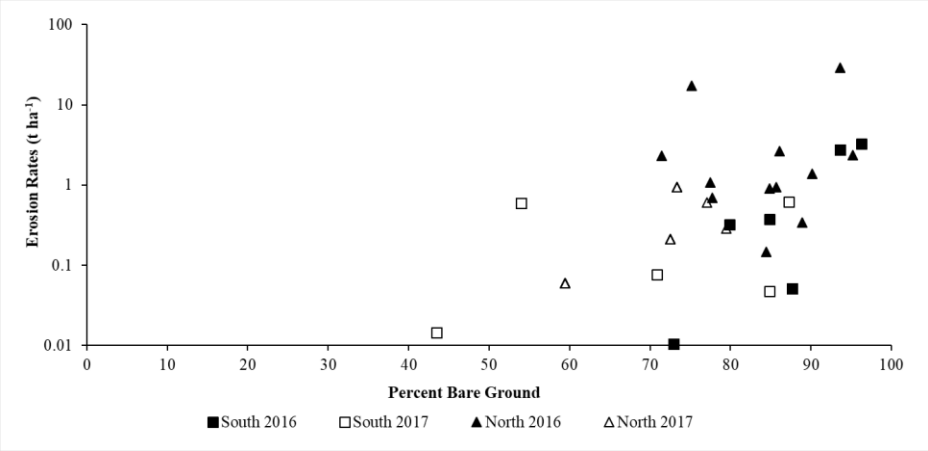

Figure 2.27. Erosion rate of the small-scale plots (short hillslope plots) and the large-scale plots (long hillslope plots and swale) compared with bare ground measured on the short vegetation plots and large vegetation plots. Only the silt fences with sediment are shown.

2.5.2 Driving Physical and Biological Attributes

The following section examines the extent to which key physical and biological attributes may explain the observed spatial and temporal variability in erosion and sediment yield throughout the Murphy Creek watershed.

2.5.2.1 Percentage of Cover

The Soda Fire consumed nearly all the vegetation across the site. The live canopy cover across the watershed was consumed leaving only burnt shrub skeletons and grass plant bases immediately following the fire in 2015 (Table 2.2).

The total ground cover immediately following the fire was similar across aspects, with the south-facing aspect being higher (Table 2.2). The greatest difference in ground cover by aspect was the difference in ash and rock cover. The north-facing aspect had the highest percentage of ground basal plant hits, ash, bare soil, and bare ground in 2015. While the south-facing aspect had the highest percentage of litter and rock ground cover in the months following the fire. The average surface roughness was lowest in 2015 with the north-facing aspect having the lowest average surface roughness (Table 2.2). This difference in canopy and ground cover in the months immediately following the fire between aspects can be explained in the difference of pre-fire vegetation and burn severity (Figure 2.28). On the south-facing aspect there was likely more sparse pre-fire vegetation and extensive rock cover which resulted in a lower burn severity in majority of the areas, and higher rock cover and limited ash compared to the north-facing aspect. Whereas, the north-facing aspect likely had greater pre-fire vegetation resulting in a higher burn severity and greater amounts of ash and bare soil relative to the south-facing aspect.

In first growing season following the fire in 2016 there was an increase in total canopy cover and a decrease in total ground cover on both aspects (Table 2.2 and 2.3). Much of this canopy cover was grass and forb cover. The shrub canopy cover remained low on both aspects in 2016 due to the lack of recovery.

The total ground cover in the first growing season decreased and was similar across aspects in 2016 (Table 2.2 and 2.3). The north and south-facing aspects had similar percentages of total ground cover in 2016 with the south-facing aspect having slightly higher. The basal plant and litter ground cover was similar across aspects, and that bare ground was mostly bare soil on both aspects in 2016. There was greater rock cover on the south-facing aspect relative to the north-facing aspect. The north-facing aspect had the highest bare soil ground cover in 2016 (Table 2.2 and 2.3). The north-facing aspect ash ground cover declined

in 2016. The average surface roughness in the first growing season increased. The average surface roughness was higher on the south-facing aspect compared to the north-facing aspect (Table 2.2).

In the second growing season post-fire in 2017 the total canopy and ground cover increased on both aspects (Figure 2.29). The north-facing aspect had the highest total canopy cover in 2017. At the large plot scale the grass canopy cover was higher on the south-facing aspect than on the north-facing aspect in 2017 (Table 2.3). At the small plot scale the grass canopy cover was greater on the north-facing aspect than on the south-facing aspect. Shrub cover remained low in the second growing season (Table 2.2).

The total ground cover increased on both aspects in the second growing season (Table 2.2 and 2.3). Total ground cover was similar for the north and south-facing aspect however, the north-facing aspect had slightly higher total ground cover at the small plot scale. The north-facing aspect had higher basal plant and bare soil ground cover than the south-facing aspect in the second growing season. The south-facing aspect had more rock and litter ground cover than the north-facing aspect in 2017. Bare ground in 2017 was similar for both aspects. However, an increase in litter cover resulted in a decline in bare ground cover on both aspects (Table 2.2 and 2.3). Ash was not present on either aspect in the second growing season. The average surface roughness in the second growing season increased. The average surface roughness was greater on the south-facing aspect than on the north-facing aspect (Table 2.2).

Figure 2.28. The Murphy Creek Watershed a month after the fire occurred. The north-facing aspect (the slope located on the left side of the image) burned at a higher severity than the south-facing aspect (the slope located on the right side of the image). The vegetation on both aspects was consumed by the fire leaving the soil surface exposed.

Table 2.1. Table of the Short Hillslope vegetation plots with the percent canopy cover and ground cover by lifeform for the time period (2015-2017). Vegetation was measured in 2015 in the months immediately following the fire and over the first and second growing period. The category in canopy cover titled other consists of forb, woody dead, and litter. The bare ground cover is comprised of bare soil cover, rock cover, and ash cover. The ground cover other category is comprised of woody dead, standing dead, moss, and dung.

Murphy Creek Watershed Short Plot Vegetation						
Canopy Cover (%)	**North**			**South**		
	2015	**2016**	**2017**	**2015**	**2016**	**2017**
Total Canopy	0.7	91.2	139.6	5.2	57.0	98.5
Shrub Canopy	0.0	0.0	0.2	0.0	0.2	1.9
Grass Canopy	0.0	21.3	64.9	0.3	10.1	44.3
Standing Dead	0.7	0.0	2.5	4.1	0.0	0.5
Other	0.0	69.8	72.0	0.9	46.6	51.9
Ground Cover (%)	**North**			**South**		
	2015	**2016**	**2017**	**2015**	**2016**	**2017**
Total Ground	34.0	16.3	47.5	37.9	10.8	36.3
Basal Plant	18.1	8.4	2.4	1.5	5.6	0.5
Litter	14.9	4.9	44.5	36.3	4.1	35.4
Ash	49.4	0.1	0.0	22.8	0.0	0.0
Bare Soil	14.6	79.0	45.2	8.7	68.8	55.6
Rock	2.0	4.6	7.2	30.5	20.4	8.0
Bare Ground	66.0	83.7	52.5	62.1	89.2	63.7
Other	1.1	1.7	0.6	0.1	1.2	0.4
Average Surface Roughness (mm)	30.0	40.0	50.0	40.0	50.0	60.0

Table 2.2. Table of the large vegetation plots (long hillslope plots and swales) with the percent canopy cover and ground cover by lifeform for the time period (2016-2017). Vegetation was measured on four transects throughout the upslope contributing area of each long hillslope plot and swale over the first and second growing period. The category in canopy cover titled other consists of forb, woody dead, and litter. The bare ground cover is comprised of bare soil cover, rock cover, and ash cover. The ground cover other category is comprised of woody dead, standing dead, moss, and dung.

Murphy Creek Watershed Large Plot Vegetation								
Canopy Cover (%)	**Swale**				**Long**			
	North		**South**		**North**		**South**	
	2016	**2017**	**2016**	**2017**	**2016**	**2017**	**2016**	**2017**
Total Canopy	82.5	129.2	110.7	121.3	84.3	138.5	99.4	117.1
Shrub Canopy	1.4	1.2	0.5	2.0	2.6	8.3	0.0	0.8
Grass Canopy	28.8	68.5	75.8	80.5	28.1	67.5	61.7	77.5
Standing Dead	0.1	0.0	0.0	0.3	0.5	0.0	0.0	0.1
Other	52.2	59.4	34.3	38.5	53.0	62.7	37.7	38.7
Ground Cover (%)	**Swale**				**Long**			
	North		**South**		**North**		**South**	
	2016	**2017**	**2016**	**2017**	**2016**	**2017**	**2016**	**2017**
Total Ground	17.8	23.4	20.8	32.8	12.7	31.1	14.6	31.3
Basal Plant	10.1	3.8	10.5	0.4	7.7	4.0	5.2	0.4
Litter	7.0	19.4	9.8	32.2	3.7	26.2	9.2	30.7
Ash	0.0	0.0	0.0	0.0	0.0	0.0	0.0	0.0
Bare Soil	68.4	69.3	55.9	48.8	79.5	65.3	53.0	44.9
Rock	17.2	7.4	23.4	18.4	7.8	3.6	32.7	23.8
Bare Ground	82.2	76.6	79.2	67.2	87.3	68.9	85.6	68.7
Other	0.7	0.1	0.4	0.1	1.4	1.0	0.3	0.1

Figure 2.29. The Murphy Creek watershed after the second growing season. The canopy cover and ground cover has had some recovery. The north has dense cover of forbs, shrubs and perennial grasses. The south facing aspect has higher amounts of ground litter cover and rock cover with the vegetation consisting of invasive plant species with some perennial grasses and forbs.

2.5.2.2 Water Repellency

In the months following the fire there was evidence of water repellency in each of the blocks on the north-facing aspect. The water repellency was strongest during this period leading into the winter months. Due to the time and weather constraints immediately after the fire the south-facing aspect was not tested for water repellency. Although water repellency on the south-facing aspect wasn't measured it's likely that this aspect had slightly water repellent areas immediately following the fire. Soils underneath burned shrubs on the south-facing aspect were likely water repellent (Pierson et al. 2009, 2011; Williams et al. 2014, 2016a).

One year after the fire the south-facing aspect still had evidence of water repellency, further suggesting there was likely strong water repellency on that aspect immediately following the fire. One year after the fire water repellency declined on the north facing aspect but was still present. In the second year following the fire, the water repellency on the south-

facing aspect dropped at the 1-3 cm depth from mineral soil surface but increased slightly at the soil surface and at depths of 4-5 cm from mineral soil surface. The north-facing aspect experienced a decline in water repellency in the second-year post-fire at all depths except at a depth of 4 cm it remained unchanged (Figure 2.30). It should be noted that water repellency was tested in a different location each year. This may have caused some variation in water repellency values due to the variation in burnt vegetation.

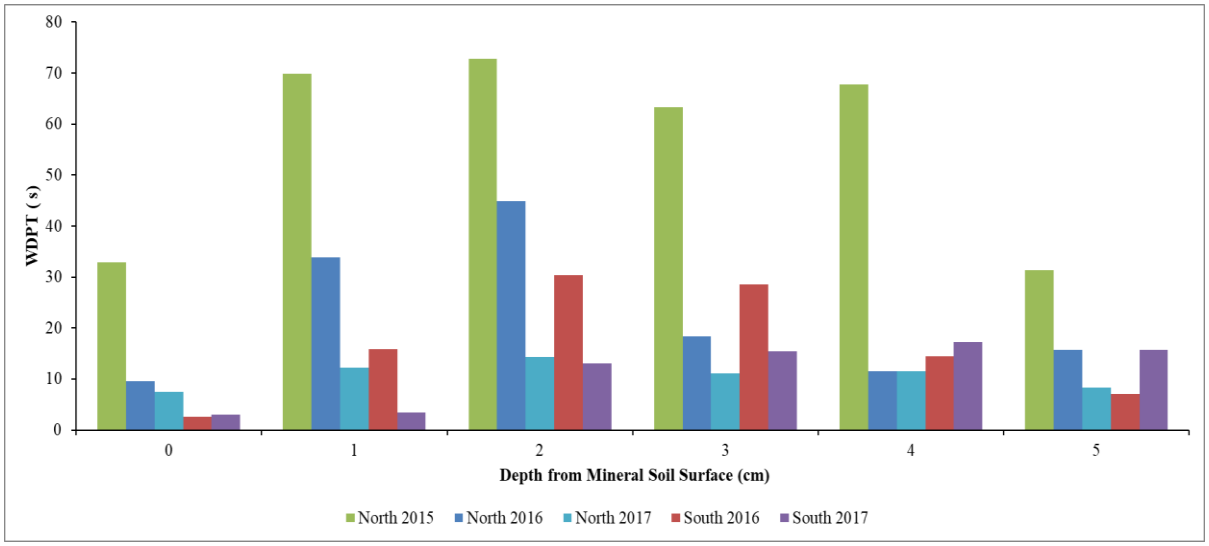

Figure2.30. Water Repellency was highest immediately following the fire. In first year post-fire both aspects had areas of high to slightly water repellent soils. In the second-year post-fire both aspects saw a decline in water repellency.

2.5.2.3 Topography

In general, the topographic analysis revealed a strong correlation between the observed spatial distribution of sediment and the topographic characteristics of the upslope contributing area. The correlation was strongest between total sediment delivered to each silt fence rather than the erosion rate (Table 2.4). The topographic correlation analysis suggests that the large swales having the greatest sediment yield could be identified using upslope contributing area, flow accumulation, topographic wetness index, stream power index, LS factor, slope steepness, and low curvature (Table 2.4).

The erosion rates had a stronger correlation to minimum and maximum values within the upslope contributing area to the silt fence rather than the areal average value of all the 3x3 m pixels which drain to the silt fence. For example, block two located on the north-facing slope above the swale had the highest contributing area, flow accumulation, topographic wetness index, stream power index, LS factor, slope steepness, and low curvature (Figure 2.31). The swale is located in a concave area and within this block is a steep exposed location with high soil erosion (Figure 2.32). The long hillslope plot in this area had less extreme topographic characteristics than the swales and was less erodible. The short hillslope plots in this area had the lowest topographic attributes but had the highest erosion rates and greatest spatial variability. As stated above, the erosion rates for the small-scale plots were 0.3 t ha^{-1} and 17.2 t ha^{-1} in the first-year post-fire. These plots are within the same proximity, yet the response of these areas is different. In this case the small-scale silt fence having the highest erosion rates also had larger values for flow accumulation, topographic wetness index, stream power index, and flow curvature. Observed and predicted canopy and ground cover life forms were also tested however the correlation was much lower than the topographic attributes.

Table 2.3. A list of the top attributes most highly correlated with total delivered sediment (t/yr) and erosion rate (t/ha).

Attributes	Year 1 Correlation Total Delivered Sediment (t/yr)	Year 2 Correlation Total Delivered Sediment (t/yr)	Year 1 Correlation Erosion Rates (t/ha)	Year 2 Correlation Erosion Rates (t/ha)
Contributing Area (Ha)	0.86	0.84	-0.19	0.49
Topographic Wetness Index Max	0.70	0.67	-0.29	0.57
Topographic Wetness Index Min	-0.65	-0.55	0.17	-0.41
Stream Power Index Max	0.79	0.82	-0.18	0.48
LS Factor Max	0.75	0.71	-0.18	0.55
Curvature Index Min	-0.79	-0.71	0.20	-0.49
Longitudinal Curvature Index Min	-0.75	-0.62	0.41	-0.46
Longitudinal Curvature Index Max	0.61	0.50	-0.13	0.25
Vertical Distance to Valley Max	0.59	0.68	-0.16	0.35
Flow Accumulation Max	0.82	0.81	-0.18	0.47
Cross Section Curvature Min	-0.77	-0.61	0.20	-0.49
Cross Section Curvature Max	0.79	0.78	-0.19	0.41
Wind Effect Max	0.58	0.65	-0.34	0.47

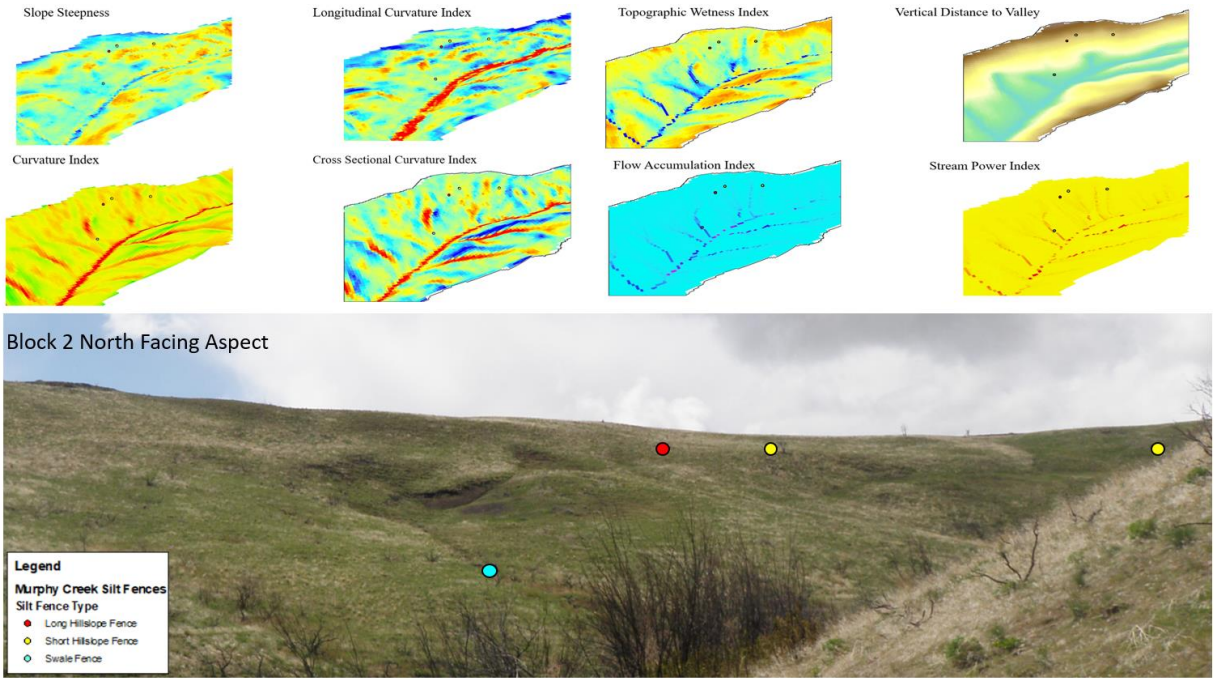

Figure 2.31. An example of how the site attributes can control spatial variability in hillslopes. The swales can be identified as areas with high slope steepness, topographic wetness index, flow accumulation, stream power index, and low curvature. Maximum values indicate areas that are most important and are reported as being areas with the most impact for that area.

Figure 2.32. Example block 2 on the north facing hillslope. Upslope depression where snow accumulated and the rill down to the beginning of the fences is shown.

2.6. Discussion

2.6.1 Post-fire Erosion Rates Across Spatial Scales

Overall the erosion and sediment delivery in this rangeland ecosystem was spatially complex and dynamic with time since wildfire. Erosion response was predominantly caused by winter snowmelt and frozen soil events. Interestingly erosion rates at the small scale were quite variable with some of the largest erosion rates measured throughout the watershed. This discussion addresses the key factors and processes that drove erosion over a two-year period.

Most of the erosion and sediment delivery occurred in the swales and was delivered in the winter months. Annual soil loss the first year following fire from forested ecosystems can range from 0.01-110 Mg ha^{-1} (Robichaud et al. 2000). In this rangeland study the annual soil loss ranged from (0-28.7 t ha^{-1}). The watershed exhibited a strong recovery over the two-year study. Interestingly, there was only a 24% increase in sediment load from year one and two (75 tons increase) despite recording more than twice the amount of streamflow. Nearly all the 2017 sediment loading took place during one peak flow event (99% of erosion occurred over a two-day period). This suggests that the deposited sediment within the watershed was relatively stable during the second year but would mobilize under extreme events. Mobilization did not occur during most of the low flow events. This implies that management strategies that reduce peak streamflow after wildfire may be successful at minimizing sediment loss from these post-fire watersheds. The swales seem to provide the hydrologic connection that delivers sediment to the stream system.

The similarity in mean annual water yield and annual precipitation relationship after wildfire (Figure 2.12) suggests that wildfire had little effect on annual streamflow from this rangeland ecosystems. In contrast to the minimal effect of wildfire on water yield, the fire greatly increased the erodibility of the hillslopes with observed sediment concentrations nearly twice as high during the first year after wildfire in comparison to those observed the second-year post-fire at the same flow rate (Figure 2.15).

Although there were not quantitative measures available, in the weeks following the fire we observed wind-blown material loading the swales and leeward hollows, mainly on the north-facing slopes. Consistently, we observed that in the winter months following the fire areas of concave topography and depressions accumulate snow and often lead to some of the highest downslope erosion rates. Based on the fact that many of these swales had large deposits of wind-blown soil, it is likely that the majority of the soil delivered in the first-year post-fire was downslope transport of wind-deposited sediments (Figure 2.33). In the second-year post-fire this trend of snowmelt-driven erosion continued, and the erosion in swales was primarily driven by rain on frozen soil and snowmelt runoff from large snow drifts. The swales consistently generated erosion on the north-facing slopes whereas, other than the head cut, the south-facing slopes consistently generated low sediment yields to the fences. Hillslopes erosion rates above the silt fences varied widely with the greatest spatially variability occurring in the short hillslope plots. The high erosion rates in the first year after the wildfire indicate that small localized erosion likely occurs throughout the watershed. The delivery of this sediment appears to be highly dependent upon how hydrologically connected small localized erosion is to a swale.

The relationship between erosion rates and upslope contributing area describes a system that is sensitive to soil deposition and storage. Based on the sediment collected in the large-scale plots (long hillslope plots and swale) and their associated contributing area, the erosion rates above the large plots was less than the erosion rates above the small-plots both years of the study. The swale sediment rates indicate that the erosion processes are likely hydrologically connected however, deposition is more likely to occur with distance down the slope as indicated by the lower sediment yield values from the large-scale plots. With the small-scale plots (short hillslope plots) there is less opportunity for soil deposition as they have a smaller contributing area. On a much larger watershed scale Vanoni (1975) described a similar trend between watershed size and the sediment delivery ratio which is the ratio of eroded sediment to sediment delivered to the watershed outlet. Vanoni (1975) notes that sediment delivery ratio typically declines with increasing drainage area. Interestingly there may be other factors which affect this relationship between sediment delivery and upslope catchment area. In a similar rangeland study Pierson et al. (2009) found in burned conditions the large-scale plots had larger erosion rates following fire than the small-scale plots.

The variation in erosion rates across spatial scales suggest the spatial connectivity within a hillslope increases once vegetation is removed. In the months immediately following the fire canopy and ground cover percentages were low and water repellency was highest. During this time the north-facing aspect had the highest percentage of ground basal plant hits, ash, bare soil, and bare ground in 2015 and the south-facing aspect had the highest percentage of litter and rock ground cover in the months following the fire. The north-facing aspect had more bare soil and strong water repellency in the months immediately following the fire. The combined bare soil and strong water repellency may explain why the north-facing aspect had more sediment delivery across plot types in the first-year post-fire.

By the first growing season in 2016 there was an increase in total canopy cover and a decrease in total ground cover on both aspects (Table 2.2 and 2.3). Bare soil at this time was highest on the north-facing aspect with the south-facing aspect having high amounts of rock and litter ground cover. There was also a decline in water repellency however, there was still evidence of hydrophobicity in the watershed. The decline in the amount of sediment delivery to north-facing short hillslope plots that was seen in the second year following the fire may be attributed to the increase in total canopy cover which provided more surface obstacles and decreased connectivity. This suggest that vegetation recovery may have had a stronger impact on the north-facing aspect due to the considerable decline in sediment delivery to the short hillslope fences. These results are similar to those reported by Williams et al. (2016b). The decline in erosion rates as vegetation and ground cover returns with time following fire observed in this study is similar to that observed in many other forested and rangeland studies (Robichaud et al. 2000; Pierson et al. 2001; Robichaud 2005; Pierson et al. 2008; Williams et al. 2016a). Based on the data collected in this study, swales located in well-vegetated north-facing slopes are the most susceptible to erosion following wildfire in these sagebrush systems. Erosion rates can be as high as 1.1 T ha^{-1} at specific locations within these north slopes. This describes a system where key local characteristics can lead to highly localized and spatial varied erosive conditions.

The hillslopes having large swales which generated high erosion were well correlated with many topographic attributes including the topographic wetness index, stream power index, LS factor, slope steepness, and curvature indices. Interestingly many of the strongest

relationships were with either the maximum or minimum value within a specific contributing area. In some cases, the sediment yield was directly related with the maximum index and indirectly with the minimum index within the same slope. For example, in the first-year post-fire the slopes having have the largest topographic wetness index were indirectly correlated to the erosion rates. This is likely due to these areas having more deposition and are areas with high localized erosion however, not all of this sediment was making it to the fences. The same year the topographic wetness index minimum was directly correlated to erosion rates. This finding suggests that even areas with lower wetness index values, such as the short hillslope plots had high erosion rates. These areas had less deposition and processes were well connected but there was overall more sediment making it to the fences at this scale. Whereas, in year two the topographic maximum was directly correlated to erosion rates and the minimum was indirectly correlated. This is likely due to sediment delivery mainly being delivered to the swales which are areas of high wetness index values. These correlations should be considered to be rough indicators as the sample size is very small.

One interesting similarity between this study and previous work was the importance of surface roughness. In a similar study conducted in burned sagebrush foothills in Boise, Idaho USA Pierson et al. (2002) compared post-fire infiltration, runoff, and inter-rill erosion on north-facing slopes and south-facing slopes in burned and unburned conditions using rainfall simulators. They found that the south-facing slopes had the highest sediment yields (>0.88 t ha^{-1}) one year following the fire. They attribute this to the south-facing slope having low surface roughness and vegetation cover needed to reduce velocity of overland flow and offer surface storage. In our study the small-scale plots on the north-facing aspect had the highest erosion rates in the first year (0.3-28.7 t ha^{-1}) and the south-facing aspect had (0-3.2 t ha^{-1}). In contrast, we found the north-facing aspect had the highest erosion rates across years and plot types (Table 2.1). In this study immediately following the fire, the average surface roughness value for all plots on the north-facing aspect was 30 mm and the south-facing aspect was 40 mm. The north-facing aspect in this study had lower surface roughness values than the south-facing aspect throughout the study period. These results suggest, that part of the reason why the north-facing aspect had the highest erosion rates was due to low surface roughness and vegetation cover in the first year following the fire. The difference in erosion rates with aspect

in the Murphy Creek watershed is also likely partly due to the high rock content on the soil surface and difference in pre-fire vegetation cover on the south-facing slopes.

One of the most novel findings of the study may be that the post-fire sediment delivery in this ecosystem occurred during the winter snowmelt period not due to intense summer storms. This finding is inconsistent with past studies. Benavides-Solorio and MacDonald (2005), performed a study in the northern Colorado Front Range and found that majority of the sediment in the silt fences was driven by high-intensity summer storms. The mean rate for summer was 16.7 Mg and in November - May sediment total was 1.2 Mg, 7% of the mean summer rate (Benavides-Solorio and MacDonald 2005). In contrast, our results showed post-fire sediment production was driven by winter processes rather than high-intensity summer storms. Another study conducted in the Colorado Front Range following fire was done by (Wagenbrenner et al. 2006). Their study assessed the effectiveness of three post-fire rehabilitation treatments in limiting erosion over a four-year period. Silt fences were used on various plot types and sediment delivery was from rain storms from May to September and not from winter process (Wagenbrenner et al. 2006). The mean sediment yield for the first-year post-fire was 11 Mg ha^{-1} and declined in the second-year post-fire to 1.2 Mg ha^{-1} (Wagenbrenner et al. 2006). The mean sediment yield from our study for all plots was 1.85Mg ha^{-1} in the first-year post-fire and 0.16 Mg ha^{-1} in the second-year post-fire. Our mean sediment yields for both years was lower than those found by Wagenbrenner et al. (2006), but we also saw a decline in mean sediment yield in the second-year post-fire.

This study suggests that the most susceptible season to post-fire erosion may occur during the winter rather than in the summer. In areas along the rain-snow transition this finding of combined wind and water processes driving erosion post-fire is not well documented. In this study we received no erosion from summer storms either year. Based on the long-term precipitation data from an analogous site (Site #095b Whisky Mountain), the summer rainfall during both years was typical for the region (Figure 2.34) (NWRC 2016, 2017). During the summer months in the two years following the Soda Fire summer storms did occur however, they did not produce any sediment.

2.6.2 Erosion Process Post-Fire in Rangelands

Since there have been few studies that have comprehensively studied post-fire erosion in the arid rangeland ecosystems we provide the following conceptual landscape level description of the primary drivers of the spatial variability based on the data we observed in this and other similar projects.

In arid rangeland ecosystems vegetation growth is primarily dependent upon soil water availability. Vegetation growth is strongest in regions where plants have access to water. In steep topography solar radiation on south-facing aspects evaporates most of the water and little soil development has occurred. On north-facing aspects snow remains longer due to lower solar radiation and sometimes more snow drifting. This excess water and in some cases, deposition of soil carried by the wind, has led to increased weathering of soil and thicker soil horizons. These thicker soil layers hold more water and allow roots to penetrate and access this stored water. As a result of these landscape level vegetation dynamics the thickest vegetative biomass generally occurs on the north-facing slopes, in springs/seeps, or near streams. Forest ecosystems compared to rangeland ecosystems often burn at a much higher severity due to the amount of fuels that have accumulated due to fire suppression and connectivity of overstory and understory fuels. The thick vegetation (overstory and understory) in forested areas and the litter layer protects the soil surface from rainsplash (Wondzell and King 2003). The litter layer also helps with infiltration and storage of water (Wondzell and King 2003).

Unlike forest ecosystems, rangeland ecosystems do not have trees so there is likely higher wind velocities which leads to more snow and soil drifting. Areas that had high amounts of vegetation pre-fire seemed to burn at a higher severity due to the amount of fuel available. Wildfire affects the hydrologic response of a rangeland landscape by increasing soil surface susceptibility to erosion and runoff (Pierson et al. 2011). At the small-plot scale the main erosion processes following fire are rainsplash and sheet flow. The consumption of protective vegetation cover increases the amount of water on the soil surface due to a decline in interception, surface water storage, and infiltration (Pierson et al. 2011). The lack of vegetation cover results in the soil surface experiencing amplified rainsplash erosion, sheet

flow, and concentrated flow (Bradford et al. 1987; Kinnell 2005; Shakesby and Doerr 2006; Al-Hamdan et al. 2012; Nouwakpo et al. 2016). At the large-plot scale the runoff and erosion responses post-fire are controlled by the amount of vegetation consumed in the fire, the surface soil, and rill erosion processes (Pierson et al. 2011). In areas where there are low amounts of ground cover, surface roughness is reduced (Pierson et al. 2011), flow easily accumulates and concentrates into continuous flow paths and increases soil erosion via rills (Nouwakpo et al. 2016). When hillslope processes are well connected and combined with bare soil, runoff and erosion increase (Williams et al. 2016b). Wildfire not only removes surface cover but can alter the topography and soil structure to the point that the dominant erosion process can change from inter-rill to rill erosion (Nearing et al. 2011).

The Soda Fire from this study is an example of the impact shrubland converted to grassland has on a fires size and severity. In our study we saw that in the first year following the fire the north-facing aspect produced the most sediment across scales compared to the south-facing aspect. The areas that were most susceptible to erosion were the north-facing swales. Erosion was driven by winter processes. The rain on snow/frozen soil combined with reduced infiltration as the result of frozen soil conditions during the winter months drove erosion in this watershed post-fire. The south-facing aspect had patchy burn severity due to shrubs present pre-fire. After the fire the vegetation patterns of the shrubs on this aspect were clearly defined. These areas would have burned at a higher severity, and likely have fire induced hydrophobicity. Pierson et al. (2002), found that following fire erosion was greatest on shrub coppice plots compared to interspace plots. On the north-facing aspect the vegetation cover pre-fire would have likely been more continuous and thicker vegetation due to the microclimate, thicker soils meaning it would have burned at a higher severity and likely had an amplified hydrophobicity or fire induced hydrophobicity. This study suggests that in steep sagebrush rangeland topography similar to Murphy Creek the largest post-fire soil erosion will occur in steep, north-facing slopes having dense vegetation before the fire. Erosion rates can be very extreme in localized topographic positions, but the delivery of the sediment will predominantly occur in topographic converging swales. The erosion rates are likely greatly increased due to post-fire wind erosion the deposits highly erodible fine sediments into these swales.

An attempt was made to classify the high erosion risk hillslopes within the larger Murphy creek watershed based on the topographic and vegetative characteristics. We prioritize landscapes with large swales as having high erodibility. We found that the swales were important features in these landscapes as they not only provided a hydrologic connection to the main stream but also collected wind transported sediment. These swales transport large amounts of sediment in the Murphy Creek watershed and therefore additional mitigation efforts should be applied to these areas. North-facing slopes eroded at much higher rates than the south-facing slopes and therefore should also be considered to be a larger risk than south-facing slopes. As a result, the north-facing hillslopes were coded as having moderate risk erosion and the swales being represented as areas of high erosion risk (Figure 2.35). Due to the south-facing short hillslope plots having minimal sediment delivery both years the south-facing hillslopes were labels as areas of low erosion risk. The south-facing swales in block one and two had the least amount of sediment both years compared to the block three swale, B3SSW. Since the majority of the south facing swales did not produce much sediment, with the exception of the head cut in B3SSW, they were labeled as low erosion risk with the exception of B3SSW. This south-facing swale consistently produced high erosion rates similar to those on the north-facing aspect and was labeled an area of high erosion risk (Figure 2.35). The swales located in the headwaters were labeled as high risk of erosion due to the type and percentage of pre-fire vegetation and topographic attributes being similar to the areas that produced high erosion rates. This sort of crude classification system suggests that extra treatment, such as applying mulch or straw bales, to these most erosive swales on the north-facing aspect should be considered.

The spatial complexity and temporal variability observed in this watershed and the limited available management based hydrologic soil erosion model suggest that there is need and opportunity to improve how models represent these landscapes. Considering the wind-blown material loading swales and the subsequent flushing of this material and erosion driven by winter processes in this burned rangeland ecosystem there are few models that have captured this type of wind process combined with winter dominated processes. There are some models that capture winter processes however, there is not currently a model that is capturing this wind process. The spatial variability observed within hillslopes and swales in

this study, is something that is not currently being considered by models. Based on the results of this study there is a lot of spatial detail that is not being considered, along with combined wind and water processes. The unique and complex findings of this study highlight the need to improve current prediction erosion models.

Figure 2.33. A series of photos showing the loading of the swales and the flushing of this wind-blown material from snow drifts upslope.

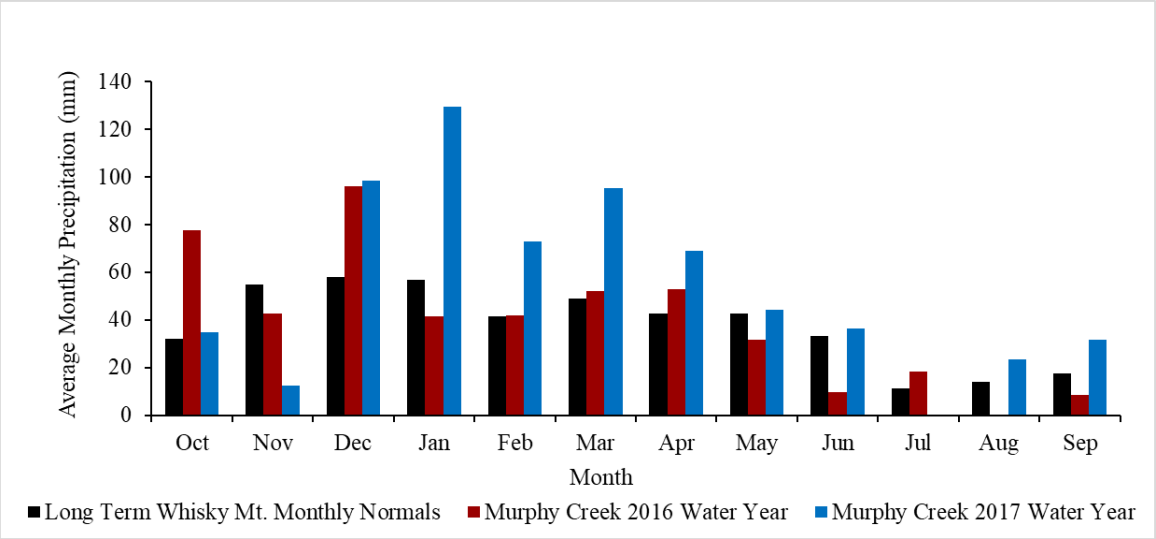

Figure 2.34. Graph showing the long-term Whisky mountain normal compared to the first and second year average monthly precipitation for Murphy Creek. In the summer months the average annual precipitation is similar to the long term monthly normal.

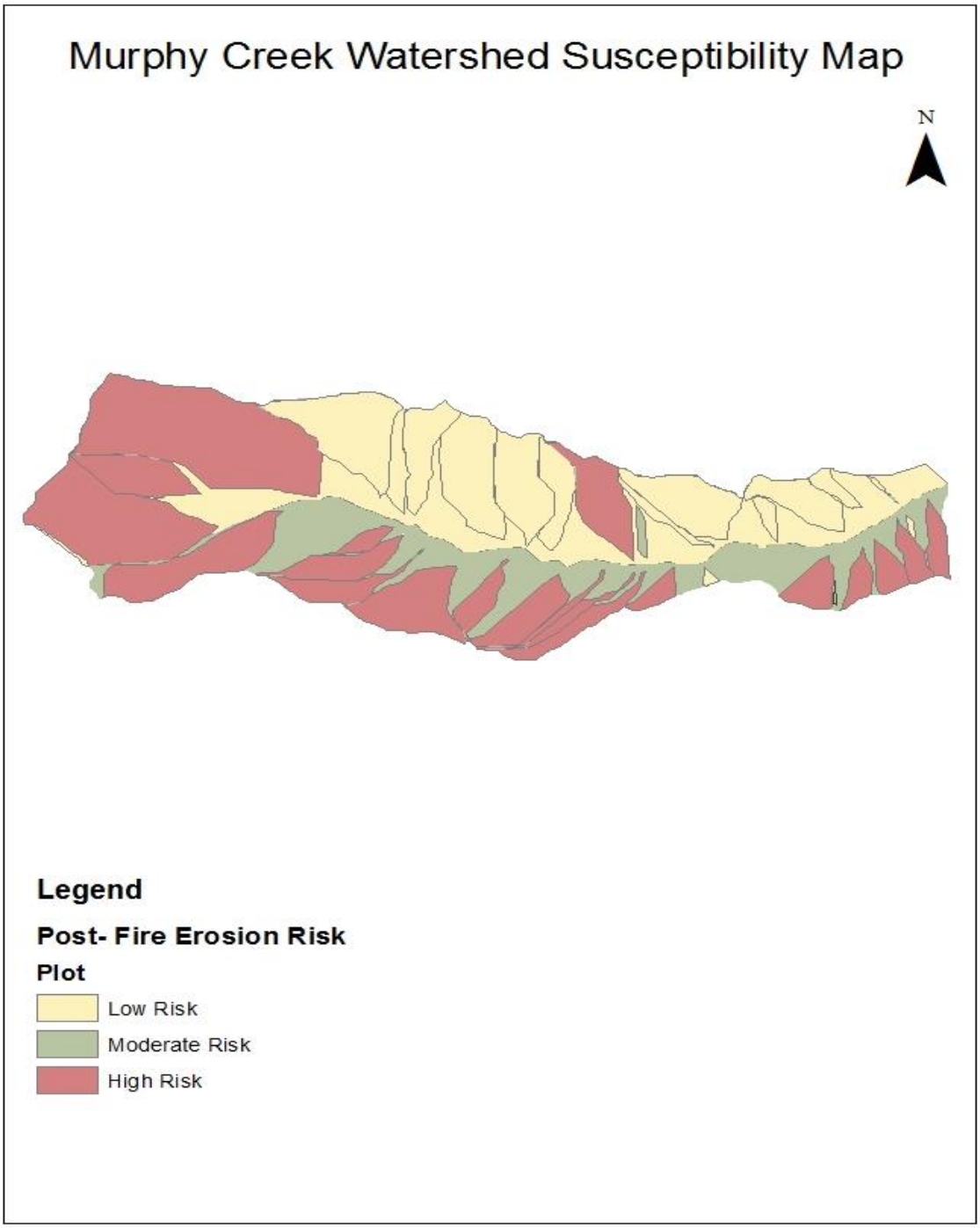

Figure 2.35. Murphy Creek Watershed Susceptibility map.

Conclusion

The results from this study highlight the importance of combined wind and water process following wildfire. In this watershed erosion varied across hillslopes and aspect. Both years following the fire erosion was driven by over winter processes. The loading of wind-blown material into swales and subsequent flushing of the swales over winter months by snowmelt and cold-season runoff can contribute considerable sediment to stream channels following burning. Consistently, we observed snow drifts in the upslope contributing area of the swales being the source of concentrated flow.

Based on the results from this study areas of high erosion risk are on the north-facing aspects in vegetated swales. These results highlight the control site characteristics have on a landscapes hydrologic and erosion response and the risk winter processes pose to burned landscapes. With scant literature on the combined wind and water processes and the unique finding of winter driven erosion the need for future research is clear. This study found that substantial erosion can be driven by combined wind and water processes post-fire. Winter processes need to be considered when making post-fire decisions and predicting post-fire erosion. More research needs to be done to improve seasonal understanding and explore modeling the impact of winter processes and loading of channels by wind.

References

Abatzoglou, J. T., & Kolden, C. A. (2011). Climate change in western US deserts: potential for increased wildfire and invasive annual grasses. *Rangeland Ecology & Management, 64*(5), 471-478.

Al-Hamdan, O. Z., Pierson, F. B., Nearing, M. A., Williams, C. J., Stone, J. J., Kormos, P. R., Boll, J., & Weltz, M. A. (2012). Concentrated flow erodibility for physically based erosion models: Temporal variability in disturbed and undisturbed rangelands. *Water Resources Research, 48*, W07504.

Al-Hamdan, O.Z., Hernandez, M., Pierson, F.B., Nearing, M.A., Williams, C.J., Stone, J.J., Boll, J., & Weltz, M.A. (2015). Rangeland hydrology and erosion model (RHEM) enhancements for applications on disturbed rangelands. *Hydrological Processes, 29*(3), pp.445-457.

Balch, J. K., Bradley, B. A., D'Antonio, C. M., & Gómez-Dans, J. (2013). Introduced annual grass increases regional fire activity across the arid western USA (1980–2009). *Global Change Biology, 19*(1), 173-183.

Benavides-Solorio, J., & MacDonald, L. H. (2005). Measurement and prediction of post-fire erosion at the hillslope scale, Colorado Front Range. *International Journal of Wildland Fire, 14*(4), 457-474.

Bisdom, E. B. A., Dekker, L. W., & Schoute, J. T. (1993). Water repellency of sieve fractions from sandy soils and relationships with organic material and soil structure. In *Soil Structure/Soil Biota Interrelationships* (pp. 105-118).

Böhner, J., & Selige, T. (2006). Spatial prediction of soil attributes using terrain analysis and climate regionalisation. *Gottinger Geographische Abhandlungen, 115*, 13-28.

Bolstad, P. (2012). *GIS Fundamentals: A First Text on Geographic Information Systems, 4th edition*. Eider Press.

Bradford, J. M., Ferris, J. E., & Remley, P. A. (1987). Interrill Soil Erosion Processes: I. Effect of Surface Sealing on Infiltration, Runoff, and Soil Splash Detachment 1. *Soil Science Society of America Journal, 51*(6), 1566-1571.

Bradley, B. A. (2009). Regional analysis of the impacts of climate change on cheatgrass invasion shows potential risk and opportunity. *Global Change Biology, 15*(1), 196-208.

Bradley, B. A., Curtis, C. A., & Chambers, J. C. (2016). Bromus response to climate and projected changes with climate change [Chapter 9]. *In: Germino, Matthew J.; Chambers, Jeanne C.; Brown, Cynthia S, eds. 2016. Exotic brome-grasses in arid and semiarid ecosystems of the western US: Causes, consequences, and management implications. Springer: Series on Environmental Management. p. 257-274.*, 257-274.

Brakensiek, D. L., Osborn, H. B., & Rawls, W. J. (1979). Field manual for research in agricultural hydrology. *Field manual for research in agricultural hydrology.239-394.*

Britton, S. L. (2001). Modeling the effectiveness of silt fence. V. *Processes,* 75.

Bryan, R. B. (2000). Soil erodibility and processes of water erosion on hillslope. *Geomorphology*, *32*(3-4), 385-415.

Chambers, J. C., Bradley, B. A., Brown, C. S., D'Antonio, C., Germino, M. J., Grace, J. B., Hardegree, S.P., Miller, R. F. & Pyke, D. A. (2014). Resilience to stress and disturbance, and resistance to Bromus tectorum L. invasion in cold desert shrublands of western North America. *Ecosystems*, *17*(2), 360-375.

Colby, B. R. (1956). *Relationship of sediment discharge to streamflow* (No. 56-27). US Dept. of the Interior, Geological Survey, Water Resources Division,.

Cooley, S. (2016). Watershed Delineation. Retrieved from http://gis4geomorphology.com/watershed/. Date Accessed: 2 April 2018

Davies, K. W., Boyd, C. S., Beck, J. L., Bates, J. D., Svejcar, T. J., & Gregg, M. A. (2011). Saving the sagebrush sea: an ecosystem conservation plan for big sagebrush plant communities. *Biological Conservation*, *144*(11), 2573-2584.

DeBano, L. F. (1981). Water-repellent soils: a state of the art. Berkeley, CA, USA: US Department of Agriculture, Forest Service. PSW-GTR-46. 21 p.

DeBano, L.F., Ffolliot, P.F., Baker, Jr M.B. (1996). Fire severity effects on water resources. In *Effects of Fire on Madrean Province Ecosystems; a Symposium Proceedings*, Ffolliot P.F., et al. *(coords*.) USDA. Forest Service Gen. Tech. Report RM-GTR-289. Rocky Mountain Forest and Range Experiment Station. Coronado National Forest. Tucson, AZ; 77–84.

Dissmeyer, G. E. (1982). How to use fabric dams to compare erosion from forestry practices. *Forestry report SA-FR; 13*.

Esri, DigitalGlobe, GeoEye, Earthstar GeographicsCNES/Airbus DS, USDA, USGS, AEX, Getmapping,Aerogrid, IGN, IGP, swisstopo, and the GIS User Community, Esri, HERE, DeLorme, MapmyIndia, © OpenStreetMap contributors.

Ffolliott, P. F., Brooks, K. N., Tapia, R. P., Chevesich, P. G., & Neary, D. G. (2013). Soil erosion and sediment production on watershed landscapes: processes and control. *UNESCO Special Technical Publication No. 32. Montevideo, Uruguay: UNESCO, International Hydrological Programme, Regional Office for Science for Latin American and the Carribbean. 73 p.*

Gessler, P. E., Moore, I. D., McKenzie, N. J., & Ryan, P. J. (1995). Soil-landscape modelling and spatial prediction of soil attributes. *International Journal of Geographical Information Systems, 9*(4), 421-432.

Glenn, Nancy. 2007. LiDAR-derived Map Products for Reynolds Creek Experimental Watershed LiDAR (1 meter, 5 meter). Boise State University, Boise Aerospace Center Laboratory. Boise, ID. http://www.idaholidar.org/data/62

Goodrich, D.C., Canfield, H.E., Burns, I.S., Semmens, D.J., Miller, S.N., Hernandez, M., Levick, L.R., Guertin, D.P., & Kepner, W.G. (2005). Rapid post-fire hydrologic watershed assessment using the AGWA GIS-based hydrologic modeling tool. In *Managing Watersheds for Human and Natural Impacts: Engineering, Ecological, and Economic Challenges* (pp. 1-12).

Havstad, K., Peters, D., Allen-Diaz, B., Bartolome, J., Bestelmeyer, B., Briske, D., Brown, J., Brunson, M., Herrick, J., Huntsinger, L., Johnson, P., Joyce, L., Pieper, Rex., Svejcar, T., & Yao, J. (2009). The western United States rangelands: A major resource. *Grassland Quietness and Strength for a New American Agriculture*, (grasslandquietn), 75-93.

Heyerdahl, E. K., Miller, R. F., & Parsons, R. A. (2006). History of fire and Douglas-fir establishment in a savanna and sagebrush–grassland mosaic, southwestern Montana, USA. *Forest Ecology and Management*, *230*(1), 107-118.

Hernandez, M., Nearing, M. A., Al-Hamdan, O. Z., Pierson, F. B., Armendariz, G., Weltz, M. A., Spaeth, K.E., Williams, C.J., Nouwakpo, S.K., Goodrich, D.C., & Unkrich, C. L. (2017). The Rangeland Hydrology and Erosion Model: A Dynamic Approach for Predicting Soil Loss on Rangelands. *Water Resources Research*, *53*(11), 9368-9391.

Herrick, J. E., Van Zee, J. W., Havstad, K. M., Burkett, L. M., & Whitford, W. G. (2005). Monitoring manual for grassland, shrubland and savanna ecosystems. Volume I: Quick Start. Volume II: Design, supplementary methods and interpretation. *Monitoring manual for grassland, shrubland and savanna ecosystems. Volume I: Quick Start. Volume II: Design, supplementary methods and interpretation.*

Ice, G. G., Neary, D. G., & Adams, P. W. (2004). Effects of wildfire on soils and watershed processes. *Journal of Forestry*, *102*(6), 16-20.

Ilangakoon, Nayani; Glenn, Nancy F.; Spaete, Lucas P.; Dashti, Hamid; and Li, Aihua. (2016). 2014 Lidar-Derived 1m Digital Elevation Model Data Set for Reynolds Creek Experimental Watershed, Southwestern Idaho [Data set]. Boise, ID:.http://doi.org/10.18122/B26C7X

Keane, R. E., Agee, J. K., Fulé, P., Keeley, J. E., Key, C., Kitchen, S. G., Miller,R., & Schulte, L. A. (2009). Ecological effects of large fires on US landscapes: benefit or catastrophe?A. *International Journal of Wildland Fire*, *17*(6), 696-712.

Kinnell, P. I. A. (2005). Raindrop-impact-induced erosion processes and prediction: a review. *Hydrological processes*, *19*(14), 2815-2844.

Knapp, P. A. (1996). Cheatgrass (*Bromus tectorum* L) dominance in the Great Basin Desert: history, persistence, and influences to human activities. *Global environmental change*, *6*(1), 37-52.

Knick, S. T., Dobkin, D. S., Rotenberry, J. T., Schroeder, M. A., Vander Haegen, W. M., & Van Riper III, C. (2003). Teetering on the edge or too late? Conservation and research issues for avifauna of sagebrush habitats. *The Condor*,*105*(4), 611-634.

Link, S. O., Keeler, C. W., Hill, R. W., & Hagen, E. (2006). Bromus tectorum cover mapping and fire risk. *International Journal of Wildland Fire*, *15*(1), 113-119.

Littell, R. C., Milliken, G. A., Stroup, W. W., Wolfinger, R. D., & Schabenberger, O. (2006). SAS for mixed model. *Cary, NC: SAS Publishing*.

Littell, J. S., McKenzie, D., Peterson, D. L., & Westerling, A. L. (2009). Climate and wildfire area burned in western US ecoprovinces, 1916–2003. *Ecological Applications*, *19*(4), 1003-1021.

Mack, R. N. (1981). Invasion of Bromus tectorum L. into western North America: an ecological chronicle. *Agro-ecosystems*, *7*(2), 145-165.

Meyer, S. E. (1994). Germination and establishment ecology of big sagebrush: implications for community restoration. *Proceedings on Ecology and Management of Annual Rangelands'. (Eds SB Monsen, SG Kitchen) USDA Forest Service, Rocky Mountain Research Station, General Technical Report RMRS-313*, 244-251.

Miller, R. F., & Tausch, R. J. (2000). The role of fire in pinyon and juniper woodlands: a descriptive analysis. In *Proceedings of the invasive species workshop: the role of fire in the control and spread of invasive species. Fire conference* (pp. 15-30).

Miller, R. F., Bates, J. D., Svejcar, A. J., Pierson Jr, F. B., & Eddleman, L. E. (2005). Biology, ecology, and management of western juniper (juniperus occidentalis). Oregon State University Agricultural Experiment Station. 77 p.

Miller, R. F., Knick, S. T., Pyke, D. A., Meinke, C. W., Hanser, S. E., Wisdom, M. J., & Hild, A. L. (2011). Characteristics of sagebrush habitats and limitations to long-term conservation. *Greater sage-grouse: ecology and conservation of a landscape species and its habitats. Studies in Avian Biology*, *38*, 145-184.

Monsen, S. B. (1994). The competitive influences of cheatgrass (Bromus tectorum) on site restoration. In Proceedings–*Ecology and Management of Annual Rangelands*. Gen Tech. Rep. INT-GTR-313. USDA, Forest Service, Intermountain Research Station, Ogden, UT (pp. 43-50).

Moody, J. A., Shakesby, R. A., Robichaud, P. R., Cannon, S. H., & Martin, D. A. (2013). Current research issues related to post-wildfire runoff and erosion processes. *Earth-Science Reviews*, *122*, 10-37.

Moore, I. D., Grayson, R. B., & Ladson, A. R. (1991). Digital terrain modelling: a review of hydrological, geomorphological, and biological applications. *Hydrological processes*, *5*(1), 3-30.

Moore, I. D., Gessler, P. E., Nielsen, G. A., & Peterson, G. A. (1993). Soil attribute prediction using terrain analysis. *Soil Science Society of America Journal*, *57*(2), 443-452.

National Cooperative Soil Survey (NCSS). (2010). LICKSKILLET SERIES. Official Series Description-LICKSKILLET Series. Retrieved from soilseries.sc.egov.usda.gov/OSD_Docs/L/LICKSKILLET.hyml. Date Accessed: 2 April 2018.

Nearing, M.A., Wei, H., Stone, J.J., Pierson, F.B., Spaeth, K.E., Weltz, M.A., Flanagan, D.C. and Hernandez, M., (2011). A rangeland hydrology and erosion model. *Transactions of the ASABE*, *54*(3), 901-908.

Nouwakpo, S. K., Williams, C. J., Al-Hamdan, O. Z., Weltz, M. A., Pierson, F., & Nearing, M. (2016). A review of concentrated flow erosion processes on rangelands: Fundamental understanding and knowledge gaps. *International Soil and Water Conservation Research*, *4*(2), 75-86.

NWRC, 2015. Public database for the Reynolds Creek Experimental Watershed. Northwest Watershed Research Center, US Department of Agriculture, Agricultural Research Service, Boise, ID, USA, Available at: ftp://ftp.nwrc.ars.usda.gov/publicdatabase/reynolds-creek/.

NWRC, 2016. Public database for the Reynolds Creek Experimental Watershed. Northwest Watershed Research Center, US Department of Agriculture, Agricultural Research Service, Boise, ID, USA, Available at: ftp://ftp.nwrc.ars.usda.gov/publicdatabase/reynolds-creek/.

NWRC, 2017. Public database for the Reynolds Creek Experimental Watershed. Northwest Watershed Research Center, US Department of Agriculture, Agricultural Research Service, Boise, ID, USA, Available at: ftp://ftp.nwrc.ars.usda.gov/publicdatabase/reynolds-creek/.

NWRC, 2018. Public database for the Reynolds Creek Experimental Watershed. Northwest Watershed Research Center, US Department of Agriculture, Agricultural Research Service, Boise, ID, USA, Available at: ftp://ftp.nwrc.ars.usda.gov/publicdatabase/reynolds-creek/.

Ott, R. L., & Longnecker, M. T. (2010). *An introduction to statistical methods and data analysis, sixth edition*. Nelson Education.

Pellant, M. (1990). The cheatgrass-wildfire cycle—are there any solutions. In *McArthur et al.(eds.) Proceedings of a Symposium on cheatgrass invasion, shrub die-off, and other aspects of shrub biology and management. US For. Serv., Int. Res. Sta., Gen. Tech. Rep. INT-276. Ogden, UT* (pp. 11-18).

Pierson, F. B., Slaughter, C. W., & Cram, Z. K. (2000). Monitoring discharge and suspended sediment, Reynolds Creek Experimental Watershed, Idaho, USA. *US Department of Agriculture, Agricultural Research Service, Northwest Watershed Research Center, Boise, ID, Technical Bulletin NWRC, 8*.

Pierson, F. B., Robichaud, P. R., & Spaeth, K. E. (2001). Spatial and temporal effects of wildfire on the hydrology of a steep rangeland watershed. *Hydrological processes*, *15*(15), 2905-2916.

Pierson, F. B., Carlson, D. H., & Spaeth, K. E. (2002). Impacts of wildfire on soil hydrological properties of steep sagebrush-steppe rangeland. *International Journal of Wildland Fire*, *11*(2), 145-151.

Pierson, F. B., Robichaud, P. R., Moffet, C. A., Spaeth, K. E., Hardegree, S. P., Clark, P. E., & Williams, C. J. (2008). Fire effects on rangeland hydrology and erosion in a steep sagebrush-dominated landscape.*Hydrological Processes*, *22*(16), 2916-2929.

Pierson, F. B., Moffet, C. A., Williams, C. J., Hardegree, S. P., & Clark, P. E. (2009). Prescribed-fire effects on rill and interrill runoff and erosion in a mountainous sagebrush landscape. *Earth Surface Processes and Landforms*, *34*(2), 193-203.

Pierson, F., Robichaud, P., Williams, J., Kormos, P., Al-Hamdan, O., & Boll, J. (2010). Use of Rainfall Simulation and Concentrated Flow Experiments to Characterize Rangeland Hydrologic and Erosional Processes in the Great Basin, USA.In *EGU General Assembly Conference Abstracts*(Vol. 12, p. 7674).

Pierson, F. B., Williams, C. J., Hardegree, S. P., Weltz, M. A., Stone, J. J., & Clark, P. E. (2011). Fire, plant invasions, and erosion events on western rangelands. *Rangeland Ecology & Management*, *64*(5), 439-449.

Pierson, F. B., & Williams, C. J. (2016). Ecohydrologic impacts of rangeland fire on runoff and erosion: A literature synthesis. *Gen. Tech. Rep. RMRS-GTR-351. Fort Collins, CO: US Department of Agriculture, Forest Service, Rocky Mountain Research Station. 110 p., 351*.

Robichaud, P.R., Beyers, J.L., & Neary, D.G. (2000). Evaluating the Effectiveness of Postfire Rehabilitation Treatments. *Gen. Tech. Rep. RMRS-GTR-63. Fort Collins, CO: U.S. Department of Agriculture, Forest Service, Rocky Mountain Research Station.* 85 p.

Robichaud, P. R., & Brown, R. E. (2002). Silt fences: An economical technique for measuring hillslope soil erosion. *Gen. Tech. Rep. RMRS-GTR-94. Fort Collins, CO: US Department of Agriculture, Forest Service, Rocky Mountain Research Station. 24 p., 94*.

Robichaud, P. R. (2005). Measurement of post-fire hillslope erosion to evaluate and model rehabilitation treatment effectiveness and recovery. *International Journal of Wildland Fire*, *14*, 475-485.

Robichaud, P. R., Elliot, W. J., Pierson, F. B., Hall, D. E., Moffet, C. A., & Ashmun, L. E. (2007a). Erosion Risk Management Tool (ERMiT) User Manual. *USDA Forest Service Rocky Mountain Research Station General Technical Report RMRS-GTR-188*, 31.

Robichaud, P. R., Elliot, W. J., Pierson, F. B., Hall, D. E., & Moffet, C. A. (2007b). Predicting postfire erosion and mitigation effectiveness with a web-based probabilistic erosion model. *Catena*, *71*(2), 229-241.

Robichaud, P.R., Ashmun, L.E., Sims, B.D. (2010a). Post-Fire Treatment Effectiveness for Hillslope Stabilization. General Technical Report, RMRS-GTR-240. U.S. Department of Agriculture, Forest Service, Rocky Mountain Research Station, Fort Collins, CO.

Robichaud, P. R., Wagenbrenner, J. W., & Brown, R. E. (2010b). Rill erosion in natural and disturbed forests: 1. Measurements. *Water Resources Research*, *46*(10).

Robichaud, P. R., & Ashmun, L. E. (2013). Tools to aid post-wildfire assessment and erosion-mitigation treatment decisions. *International Journal of Wildland Fire. 22: 95-105.*, 95-105.

Romme, W. H., Allen, C. D., Bailey, J. D., Baker, W. L., Bestelmeyer, B. T., Brown, P. M., Eisenhart, K.S., Floyd, M.L., Huffman, D.W., Jacobs, B.F. & Miller, R. F. (2009). Historical and modern disturbance regimes, stand structures, and landscape dynamics in pinon–juniper vegetation of the western United States. *Rangeland Ecology & Management*, *62*(3), 203-222.

Runkel, R. L., Crawflord, C. G., & Cohn, T. A. (2004). Load estimator (LOADEST): A FORTRAN program for estimating constituent loads in streams and rivers. US Geol. Survey Techniques and Methods, Book 4, Chapter A5. USGS, Reston, VA. *https://pubs.usgs. gov/tm/2005/tm4A5/pdf/508final.pdf (verified 16 June 2009). USGS, Reston, VA*.

SAS Institute Inc. 2013. SAS version 9.4. SAS Institute, Inc.: Cary, NC.

Seyfried, M. S., Harris, R. C., Marks, D., & Jacob, B. (2000). A geographic database for watershed research, Reynolds Creek Experimental Watershed, Idaho, USA. *Tech. Bull. NWRC 2000*, *3*, 26.

Seyfried, M., Harris, R., Marks, D., & Jacob, B. (2001). Geographic database, Reynolds Creek Experimental Watershed, Idaho, United States. *Water Resources Research, 37*(11), 2825-2829.

Shakesby, R. A., & Doerr, S. H. (2006). Wildfire as a hydrological and geomorphological agent. *Earth-Science Reviews, 74*(3-4), 269-307.

Shaw Fabric Products. (n.d.) Fabric Specifications. Retrieved from http://shawfabricproducts.com/Framify.php?Page=Home.php.

Sherwood, W. C., & Wyant, D. C. (1976). *Installation of straw barriers and silt fences* (No. VHTRC 77-R18). Virginia Transportation Research Council.

Simanton, J. R., Johnson, C. W., Nyhan, J. W., & Romney, E. M. (1986). Rainfall simulation on rangeland erosion plots. In *Proceedings of the Rainfall Simulator Workshop. Tucson, AZ. January* (pp. 14-15).

Slaughter, C. W., Marks, D., Flerchinger, G. N., Van Vactor, S. S., & Burgess, M. (2001). Thirty-five years of research data collection at the Reynolds Creek Experimental Watershed, Idaho, United States. *Water Resources Research, 37*(11), 2819-2823.

Smith, H. G., Sheridan, G. J., Lane, P. N., Nyman, P., & Haydon, S. (2011). Wildfire effects on water quality in forest catchments: a review with implications for water supply. *Journal of Hydrology, 396*(1), 170-192.

Spigel, K. M., & Robichaud, P. R. (2007). First-year post-fire erosion rates in Bitterroot National Forest, Montana. *Hydrological Processes, 21*(8), 998-1005.

Stephenson, G. R. (1977). Soil-geology-vegetation inventories for Reynolds Creek Watershed, Miscellaneous series No. 42, Agricultural Experiment Station, University of Idaho College of Agriculture.

Tausch, R. J. (1999). Historic pinyon and juniper woodland development. *Proceedings: ecology and management of pinyon–juniper communities within the Interior West. Ogden, UT, USA: US Department of Agriculture, Forest Service, Rocky Mountain Research Station, RMRS-P-9*, 12-19.

Theisen, M. S. (1992). The role of geosynthetics in erosion and sediment control: An overview. *Geotextiles and Geomembranes, 11*(4-6), 535-550.

United States Department of Interior, Bureau of Land Management (USDI BLM). 2015. NOTICE OF DISTRICT MANAGERS FINAL DECISION Soda Fire Emergency Stabilization and Rehabilitation Plan Boise and Vale District Offices, Bureau of Land Management. Retrieved from https://eplanning.blm.gov/epl-front-office/projects/nepa/52963/64613/70005/soda_decision_FINAL101915_electronicsig_binder.pdf

USDA-FSA-APFO Aerial Photography Field Office. (2016a). SOLDIER CAP, SE. NAIP Digital Ortho Photo Image. USDA-FSA-APFO Aerial Photography Field Office, Salt Lake City, UT. Date Accessed: 30 January 2018.

USDA-FSA-APFO Aerial Photography Field Office. (2016b). SOLDIER CAP, SW. NAIP Digital Ortho Photo Image. USDA-FSA-APFO Aerial Photography Field Office, Salt Lake City, UT. Date Accessed: 30 January 2018.

USGS EROS. 2015. Soda fire, located about 40 miles southwest of Boise, ID. Raster digital data. Sioux Falls, South Dakota USA: U.S. Geological Survey. Retrieved from http://edc.usgs.gov

Vanoni, V. A. (1975). Sedimentation engineering, ASCE manuals and reports on engineering practice—No. 54. *American Society of Civil Engineers, New York, NY*.

Wagenbrenner, J. W., MacDonald, L. H., & Rough, D. (2006). Effectiveness of three post-fire rehabilitation treatments in the Colorado Front Range. *Hydrological processes, 20*(14), 2989-3006.

West, N. E. (1999). Juniper–pinon savannas and woodlands of western North America. In R. C. Anderson, J. S. Fralish, & J. M. Baskin (Eds.), *Savanna, barrens, and rock outcrop plant communities of North America* (pp. 288−308). Cambridge: Cambridge University Press.

Whisenant, S. G. (1990). Changing fire frequencies on Idaho's Snake River plains: ecological and management implications. In: E. D. McArthur, E. M. Romney, S. D. Smith, and P. T. Tuellar [EDS.]. Proceedings: Symposium on Cheatgrass Invasion, Shrub Dieoff, and Other Aspects of Shrub Biology and Management: 5–7 April 1989; Las Vegas, NV, USA. General Technical Report INT-276. Ogden, UT, USA: US Department of Agriculture, Forest Service, Forest Service Intermountain Research Station. p. 4–10.

Williams, C. J., Pierson, F. B., Robichaud, P. R., & Boll, J. (2014). Hydrologic and erosion responses to wildfire along the rangeland–xeric forest continuum in the western US: a review and model of hydrologic vulnerability. *International journal of wildland fire*, *23*(2), 155-172.

Williams, C. J., Pierson, F. B., Kormos, P. R., Al-Hamdan, O. Z., Hardegree, S. P., & Clark, P. E. (2016a). Ecohydrologic response and recovery of a semi-arid shrubland over a five year period following burning. *Catena*, *144*, 163-176.

Williams, C. J., Pierson, F. B., Robichaud, P. R., Al-Hamdan, O. Z., Boll, J., & Strand, E. K. (2016b). Structural and functional connectivity as a driver of hillslope erosion following disturbance. *International Journal of Wildland Fire*, *25*(3), 306-321.

Wilson, J. P., & Gallant, J. C. (2000). Secondary topographic attributes. *Terrain analysis: Principles and applications*, 87-131.

Wondzell, S. M., & King, J. G. (2003). Postfire erosional processes in the Pacific Northwest and Rocky Mountain regions. *Forest Ecology and Management*, *178*(1-2), 75-87.